Decoupling interfacial processes in the formulation of fluorine-free lithium metal batteries

Amy S. Metlay,[1] Susie Park,[1] Sophia C. Bracco,[2] Lauren E. Marbella[1,*]

[1]Department of Chemical Engineering, Columbia University, New York, NY 10027 USA

[2]Department of Chemistry, Barnard College, Columbia University, New York, New York 10027, USA

Contents

Materials

Lithium hexafluorophosphate ($LiPF_6$, ≥99.99%), lithium nitrate ($LiNO_3$, ≥99.9%), and lithium bis(oxalate)borate (LiBOB) were purchased from Sigma Aldrich and dried at ~90 °C under vacuum using a Schlenk line before transferring and storing in an argon-filled glovebox (O_2 < 0.1 ppm, H_2O < 0.5 ppm). Ethylene carbonate (EC, ≥99%) and 1,2-dimethoxyethane (DME, 99.5%) were purchased from Sigma Aldrich and stored in an argon filled glovebox. CR2032 coin cell fabrication materials (stainless steel tops, bottoms, 0.5 mm spacers, Belleville washer springs) were purchased from MTI corporation and dried overnight in a 60 °C oven prior to use. Lithium foil (0.7 mm thickness, MF-Li25) was also purchased from MTI Corporation. Microporous trilayer membranes (25 μm thickness, 2325-Celgard) purchased from Celgard and glass microfiber filters (260 μm thickness, Whatman) were used as separators in coin cells and treated at 60 °C. Copper (0.321 mm diameter, Remington Industries), tungsten (0.025 mm diameter, Goodfellow), and lead-free soldering (0.6 mm diameter, Mandala Crafts) wires were used for ultramicroelectrode (UME) fabrication. Epoxy (Permatex 84201) was purchased from Amazon. All materials were stored in an argon-filled glovebox unless specified otherwise.

Battery Fabrication

Symmetric Li||Li cells were fabricated following the assembly order depicted in supporting Figure S1a. Li foil was punched into 12 mm diameter discs. Separators were punched into 12.7 mm discs and were used for all symmetric cell experiments. Li||Cu half cells were fabricated following the order depicted in supporting Figure S1b. Li foil was punched into 12 mm diameter discs, Cu foil was punched into 19 mm diameter discs, and separators were punched into 19 mm diameter discs. Glass microfiber separators were used for all reported electrochemistry experiments, and Celgard separators were used for all characterization experiments (see below).

Ultramicroelectrode Fabrication

Ultramicroelectrodes were fabricated by soldering 25 μm diameter tungsten wire to 250 μm diameter Cu wire. The soldered wire was then threaded through a cut 1 mL plastic pipette such that the tungsten was exposed at the original small opening of the pipette and the copper was exposed at the larger newly cut opening of the pipette (Fig. S2). The wire was secured in place using epoxy and allowed to partially set for ~1 h before transferring to a 60 °C oven overnight to fully cure. After fully curing, the small end of the pipette was cut such that the tungsten wire was perfectly flushed with the epoxy/pipette assembly. Prior to each experimental use, the electrode was cleaned by sanding and sonicating in deionized water and isopropyl alcohol.

Ultramicroelectrodes were used to ensure no voltammogram distortion due to the electrode cell time constant, $\tau = R_s C_{dl}$ where τ represents the time it takes for the non-faradaic component of the electrode to charge, R_s is solution resistance, and C_{dl} is the double layer of the electrode. To avoid distortion, experimental time length should exceed $5\times\tau$.[1]

Electrochemical Measurements

Transient cyclic voltammetry (CV) was acquired using a scan rate of 10 V/s on a Gamry Interface 1010e instrument using a UME working electrode vs lithium reference/counter electrode two-electrode setup akin to that used by Boyle and coworkers.[2] The first plating/stripping cycle (swept from 2.5 V to -1.2 V vs. Li/Li^+) was used in the charge transfer analysis to ensure no lithium buildup on the electrode. UMEs were cleaned prior to each cyclic voltammetry sweep.

Coulombic efficiency (CE) was measured by cycling Li||Cu half cells on an Arbin battery cycler at 0.5 mA/cm^2 for 1 h for 100 plating/stripping cycles. Cells used for SEM and XPS characterization were also cycled on the Arbin instrument at 0.5 mAh/cm^2 for specified durations.

Electrochemical impedance spectroscopy (EIS) measurements on Li||Li symmetric cells were run using a Biologic MPG-200 instrument. Two different EIS methodologies labeled as ePEIS and nPEIS were used in this study. In ePEIS measurements, potentiostatic EIS was taken at 0 V vs. open circuit voltage (OCV) with a 10 mV amplitude from 100 kHz to 1 Hz. EIS measurements were taken every 10 min during the first 1 mA/cm^2 charging period with a 1 min rest between constant current and EIS scans such that six EIS measurements were collected and 1 mAh/cm^2 capacity was applied to the cell. In nPEIS measurements, potentiostatic EIS was taken at 0 V vs. OCV with a 10 mV amplitude from 100 kHz to 1 Hz. Scans were taken every 5 h for a total of 14 EIS scans over 65 h. A simple Randle's circuit was used to fit Nyquist plots between 100 kHz to 10 Hz using the AfterMath fitting software. Fitted values of R from the RC component of the Randle's circuit represent the charge transfer/SEI transport resistance.

Nuclear Magnetic Resonance Spectroscopy

Solution NMR samples were prepared in an Ar-filled glovebox by filling a 3.65 mm outer diameter fluorinated ethylene propylene (FEP) tube with 300 µL of sample. This tube was snuggly placed in a 5 mm outer diameter glass J-young tube containing roughly 100 µL of DMSO-d_6 used for locking, shimming, and chemical shift referencing (see below).

^7Li NMR measurements used to probe Li^+ solvation environments were recorded on a 60 MHz benchtop X-Pulse NMR spectrometer (Oxford Instruments). Spectra were collected using a 90° pulse, 8 scans, and a relaxation delay of $5\times T_1$ as determined through an inversion recovery

experiment and referenced to LiCl at 0 ppm (Table S4). Due to the external locking capabilities of the X-Pulse, the instrument was locked externally and shimmed with a 20% chloroform in acetone-d_6 standard prior to experimentation that is separate from the electrolyte sample. Therefore, all solvation environment shifts were measured using the same shimming environment.

^{19}F, ^{17}O, and variable temperature ^{7}Li NMR spectra were collected on a Bruker Avance III 400 MHz spectrometer equipped with a triple resonance broadband observe (TBO) probehead. For ^{19}F NMR, at least 32 scans were acquired at room temperature using a 90° pulse and a recycle delay of 1 s. Chemical shifts were internally referenced to the PF_6^- doublet at -73 ppm. For ^{17}O NMR, over 5120 scans were acquired at room temperature using a 90° pulse and a recycle delay of 0.01 s. Chemical shifts were referenced to water at 0 ppm.

Scanning Electron Microscopy

SEM images of Cu foils after 4 hours of 1 mA/cm^2 plating were taken using a Zeiss Sigma VP SEM at 5 kV EHT at specified magnification values. Before imaging, copper electrodes were extracted from the coin cell and washed with DME in an argon filled glovebox before drying under vacuum overnight. Cut pieces of the remaining SEI/lithium composite on the Cu electrode were subsequently mounted on the SEM sample holder using double sided carbon tape. The sample holder was placed in an airtight container before transfer into the SEM chamber, resulting in <10 s of sample exposure to ambient conditions.

XPS Measurements

Li||Cu half cells were cycled at 0.5 mAh/cm^2 for 20 cycles and testing was ended by stripping Li off of Cu to 1 V vs Li/Li$^+$. The Cu electrode was then harvested from the cell and thoroughly washed in DME before drying under vacuum. Fluorine containing samples (PF_6^-, PN, PB) were dried in the glove box antechamber overnight. The dry samples were mounted on the XPS sample holder and transferred into the XPS intro chamber using an air-free transfer vessel, allowing zero exposure time to the ambient atmosphere. Fluorine-free samples (BOB^-, NO_3^-, BN) were first slightly dried with a small hand-held electric fan before mounting on the XPS sample holder and being introduced to the XPS intro chamber where they were subsequently dried under vacuum overnight. Different drying methods for fluorine containing and fluorine free samples were utilized to minimize the chance of contamination of the fluorine-free samples with fluorinated vapors in the glovebox.[3]

Measurements were run on a PHI VersaProbe II XPS spectrometer with a monochromatic Al X-ray source set at 50 W power and 15 kV accelerating voltage with pass energies of 117.4 eV (survey scan), and 29.35 eV (high resolution scans for C 1s, N 1s, O 1s, Li 1s, F 1s, B 1s, Cu

2p3, and P 2p). Spectra were referenced to adventitious carbon at 284.8 eV using the Multipak analysis software. Atomic composition analyses and high-resolution peak fitting were performed using the Multipak software.

Statistical Analysis of XPS Compositional Data

We ran a cosine similarity analysis to determine the similarity between the specific XPS-determined compositions (Tables S7-S13) of the six analyzed electrolyte formulations using the following equation 1:

$$similarity = \frac{x \cdot y}{\|x\|\|y\|} \quad \text{(eq. 1)}$$

Where x and y are vector representations of the percent composition breakdown of the SEI of cells "x" or "y".

Exchange Current Density Calculations

A Butler-Volmer approximation[1] holds and is used for electrochemical analyses at low overpotential regions.[4] Thus,

$$j = j_0\left[e^{(1-\alpha)f\left(E-E_{eq}\right)} - e^{-\alpha f\left(E-E_{eq}\right)}\right] \quad \text{(eq. 3)}$$

where j is current density, j_0 is exchange current density (here used to describe reaction rate), α is the charge transfer coefficient, E is working potential, E_{eq} is equilibrium potential, and f is (F/RT) or Faraday's constant divided by the universal gas constant and temperature. Following the mathematical approximation where for small values of x

$$e^x \to 1 + x \quad \text{(eq. 4)}$$

at low overpotential values were ($E-E_{eq}$) is small, the Butler-Volmer equation becomes

$$j = j_0\left[1 + (1-\alpha)f\left(E - E_{eq}\right) - 1 + \alpha f\left(E - E_{eq}\right)\right] \quad \text{(eq. 5)}$$

Which simplifies to

$$j = -j_0 f \eta \quad \text{(eq. 6)}$$

where η is overpotential. Following the relationship between current, potential, and resistance

$$R_{ct} = {}^{RT}/_{F j_0} \quad \text{(eq. 7)}$$

Where R_{ct} is charge transfer resistance. We divide values of R_{CT} derived from equivalent circuit fittings of EIS Nyquist plots by 2 prior to input into equation 7 to account for the symmetry and equal contribution of both working and counter electrodes in the symmetric Li||Li cell setup.

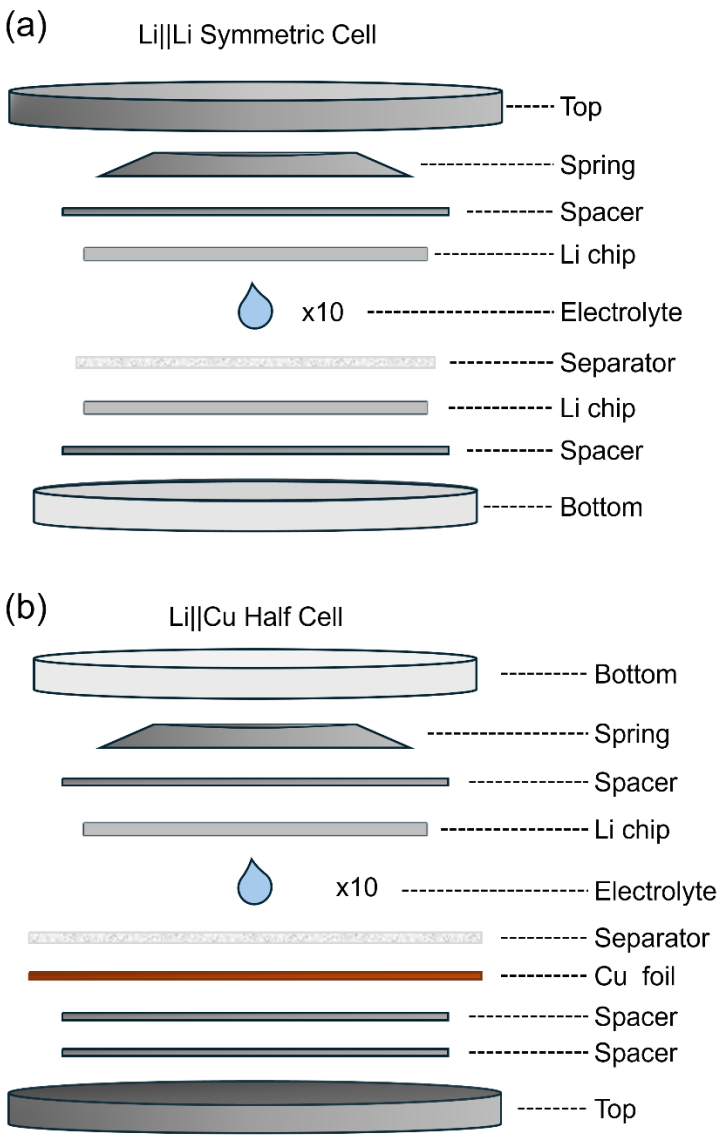

Figure S1. Coin cell assembly diagrams of (a) Li||Li symmetric cells and (b) Li||Cu half cells. Cells were constructed following the order from bottom to top of the diagrams.

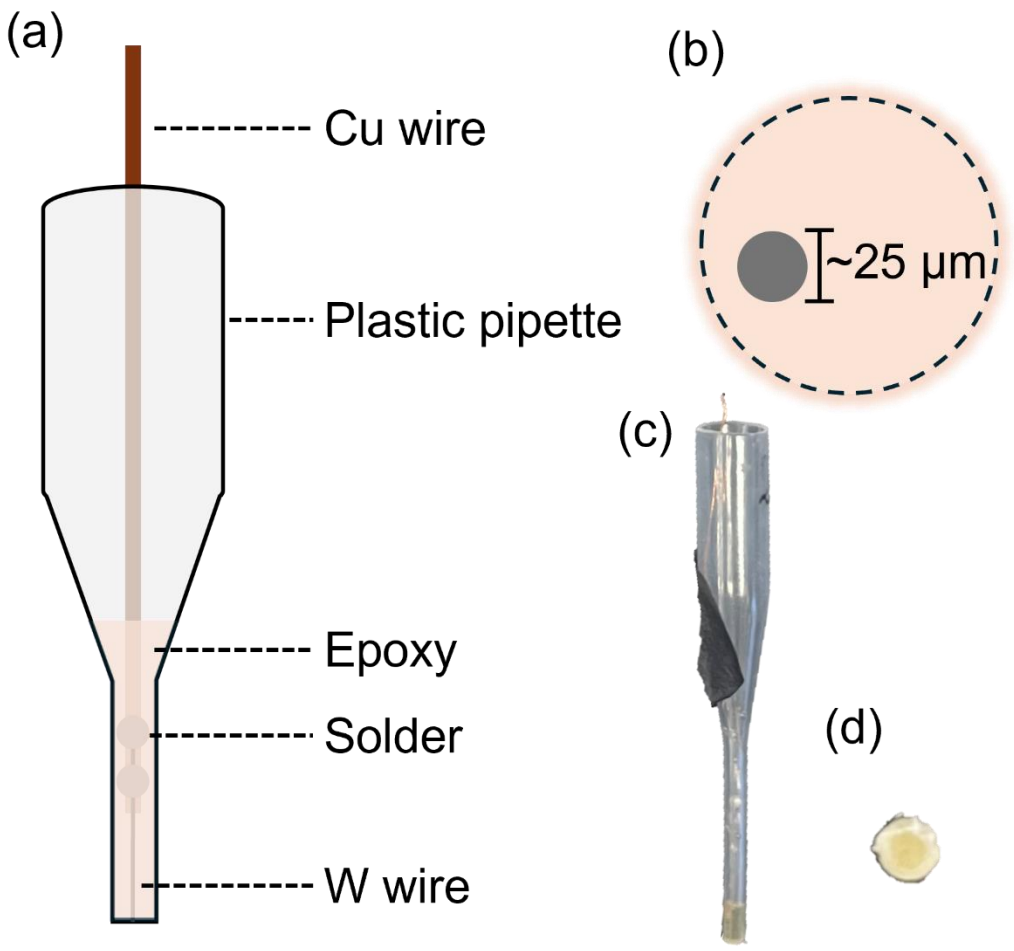

Figure S2. Ultramicroelectrode (a) cartoon diagram of assembly from a side view and (b) top-down view with a tungsten wire dimension of 25 µm. Photos of (c) a side view and (d) top-down view of a real ultramicroelectrode.

Table S1. ^{7}Li NMR shifts of samples in 1:1 EC/DME

Peak shift of the solvated Li^+ peak as shown in ^{7}Li NMR conducted on a 60 MHz instrument. The internal temperature of the instrument is 40 °C. Values are referenced to LiCl at 0 ppm.

Sample	δ Li^+ (ppm)
PF_6^-	-1.45
BOB^-	-1.41
NO_3^-	-0.60
1:1 PB	-1.42
1:1 PN	-0.95
1:1 BN	-0.93

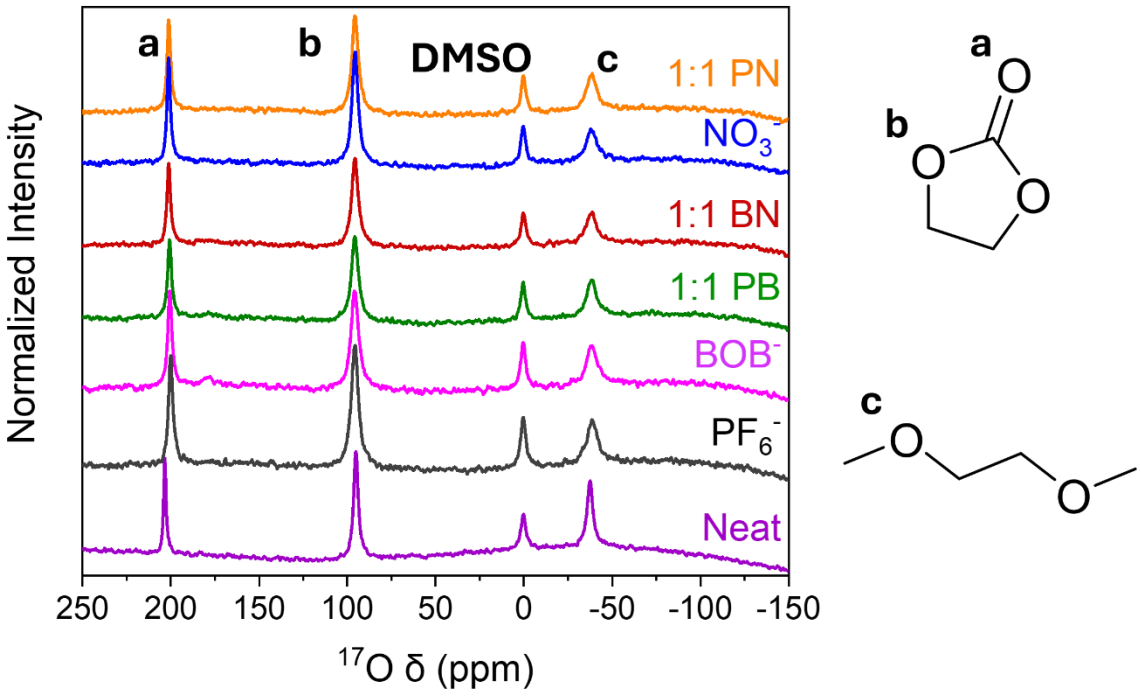

Figure S3. Full ^{17}O NMR spectra taken of the electrolyte series on a 400 MHz instrument. Assigned oxygen peaks are (a) EC carbonyl, (b) the EC ether, and (c) the DME ether. All spectra are referenced to water at 0 ppm.

Table S2. ^{17}O NMR shifts of samples

Peak shifts of the solvent oxygens as shown by ^{17}O NMR conducted on a 400 MHz instrument at room temperature. Values outside of parentheses represent the absolute shift relative to the water reference (0 ppm). Values inside of parentheses represent the change in shift relative to the neat electrolyte.

Sample	δ EC carbonyl (shift from neat)	δ EC ether (shift from neat)	δ DME ether (shift from neat)
Blank	218.58 (0)	110.57 (0)	-22.21 (0)
PF_6^-	215.33 (-3.25)	110.82 (0.25)	-22.71 (-0.50)
BOB^-	215.83 (-2.75)	111.32 (0.75)	-22.71 (-0.50)
NO_3^-	216.58 (-2.00)	110.82 (0.25)	-22.46 (-0.25)
1:1 PB	216.08 (-2.50)	111.07 (0.50)	-23.20 (-1.00)
1:1 PN	216.58 (-2.00)	111.07 (0.50)	-23.46 (-1.25)
1:1 BN	216.58 (-2.00)	110.82 (0.25)	-23.46 (-1.25)

Table S3. ^{17}O NMR EC Carbonyl FWHM

FWHM and peak area of the EC carbonyl peak from ^{17}O NMR spectra collected on a 400 MHz instrument at room temperature. The peak areas are normalized with respect to BOB^-. This normalized peak area is used to scale the FWHM value to account for slight differences between electrolyte concentration, shim, etc. that could lead to differences in FWHM.

Sample	EC carbonyl Normalized area	EC carbonyl Scaled FWHM (Hz)
Blank	--	91.7
PF_6^-	1.10	136.6
BOB^-	1	150.4
NO_3^-	1.16	102.1
1:1 PB	0.95	146.1
1:1 PN	1.06	118.6
1:1 BN	0.95	128.4

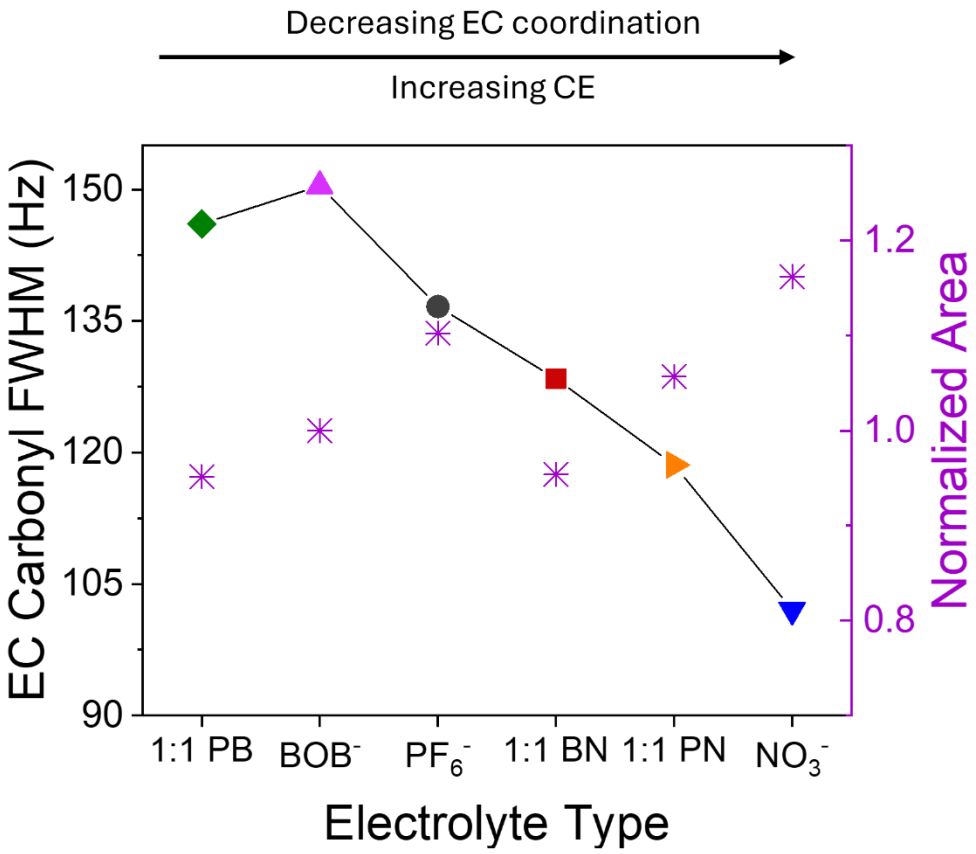

Figure S4. Area of the EC carbonyl peak in ^{17}O NMR experiments normalized with respect to LiBOB plotted as purple stars against the right y-axis. FWHM values of the EC carbonyl peak are scaled by this normalized value and are plotted against the left axis.

Table S4. ^{7}Li NMR T_1 values

Values of T_1 for the Li^+ ^{7}Li NMR peak in the different electrolytes as determined by an inversion recovery experiment. 5*T_1 was used as the recycle delay for all ^{7}Li NMR experiments.

Sample	T_1 60 MHz NMR (s)
PF_6	4.1
BOB	5.6
NO_3	3.3
1:1 PB	4.5
1:1 PN	2.2
1:1 BN	3.9

Supplementary Note 1: Analysis of FWHM of ^{17}O NMR

To further probe the coordinated-to-free solvent ratio in our electrolyte formulations, we conduct a FWHM analysis of the EC carbonyl oxygen peak in ^{17}O NMR (Table S3). Due to the quadrupolar nature of NMR, we expect that the FWHM value to be particularly sensitive to interactions with Li^+, where line broadening indicates decreased molecular mobility and longer residence time in the solvation shell. We selected EC carbonyl oxygen environment due to the relatively large magnitude of peak shift it experiences upon solvation of the Li^+ cation, indicating that it is the primary sight of solvent coordination in the Li^+ solvation sphere. Figure S4 shows the calculated FWHM and normalized areas of the EC carbonyl peak for the electrolyte series. The displayed FWHM is scaled by the normalized area of the EC carbonyl peak for each electrolyte type to account for slight discrepancies in electrolyte concentration, shimming, and locking conditions. We see that across the electrolyte series, the FWHM of the EC carbonyl peak decreases as an approximate function of solvent population in the Li^+ solvation shell, with pure LiBOB, 1:1 PB, and pure $LiPF_6$ displaying the largest FWHM values at 150 Hz, 146 Hz, and 137 Hz, respectively. We expect FWHM to decrease as a function of mobility of the probed environment. In other words, free and highly mobile EC molecules should have a smaller ^{17}O NMR EC carbonyl peak FWHM than that of the coordinated EC carbonyl peak due to the increased mobility of a non-coordinated solvent. Accordingly, the FWHM of the EC carbonyl peak in neat EC:DME is significantly smaller than the FWHM of the peak in any of the analyzed electrolytes at a measured value of 92 Hz (Table S3). Thus, the large FWHM present in pure LiBOB, 1:1 PB, and pure $LiPF_6$ indicates that a significant portion of the EC population in the electrolyte is coordinated to the Li^+ cation. In nice agreement with the results from our above peak shift analysis, addition of the NO_3^- anion consistently results in a decreased FWHM with the pure $LiNO_3$ displaying the smallest FWHM, followed by 1:1 PN and then 1:1 BN at 102 Hz, 119 Hz, and 128 Hz respectively, indicating that pure $LiNO_3$ has the highest displacement of EC in the Li^+ solvation shell, followed by 1:1 PN and then 1:1 BN.

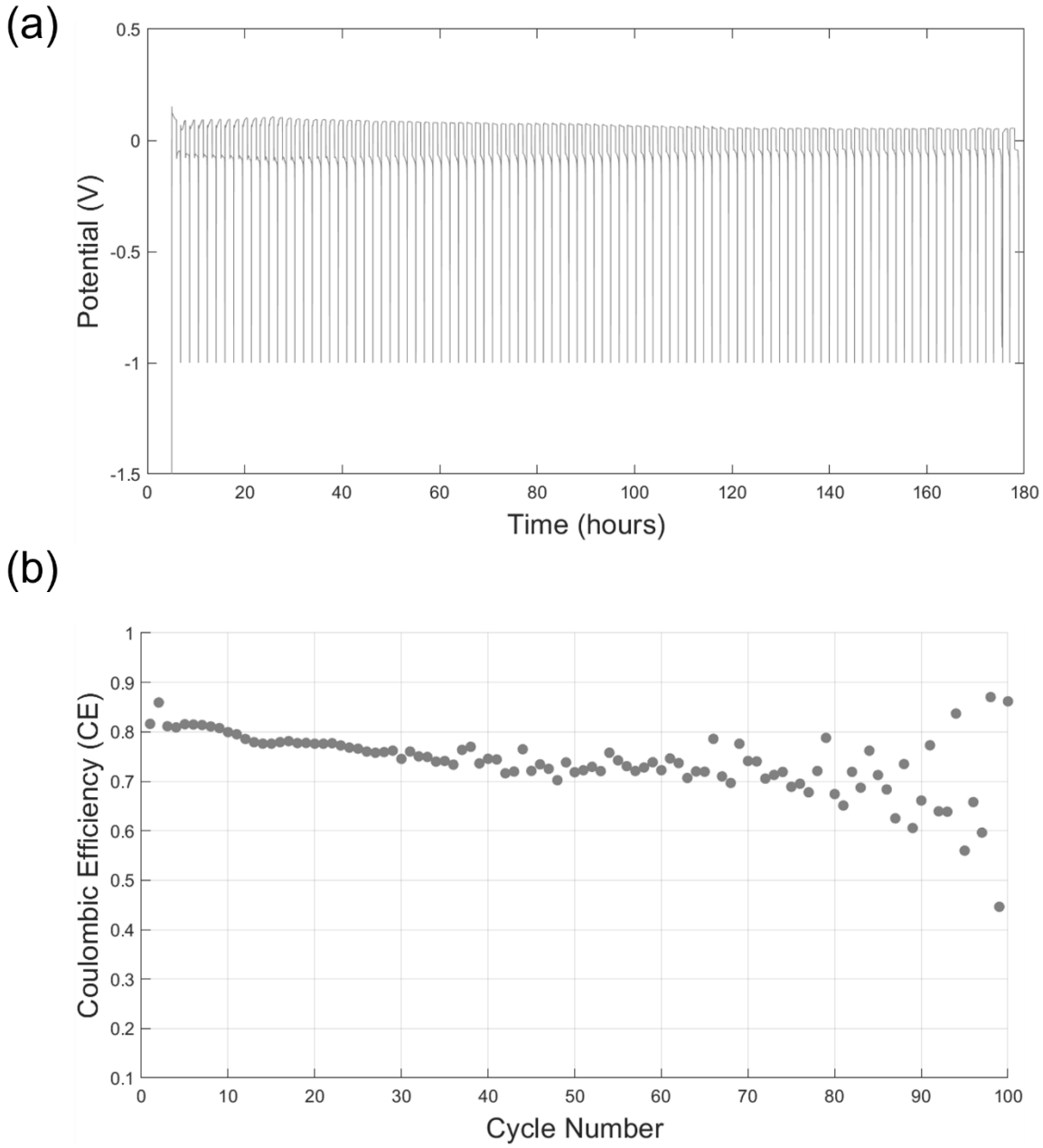

Figure S5. Example data of (a) voltage vs. time charging profile and (b) per cycle CE of a PF_6^- cell used to calculate average CE shown in Figure 1. At least three cells are used to tabulate the values in Figure 1.

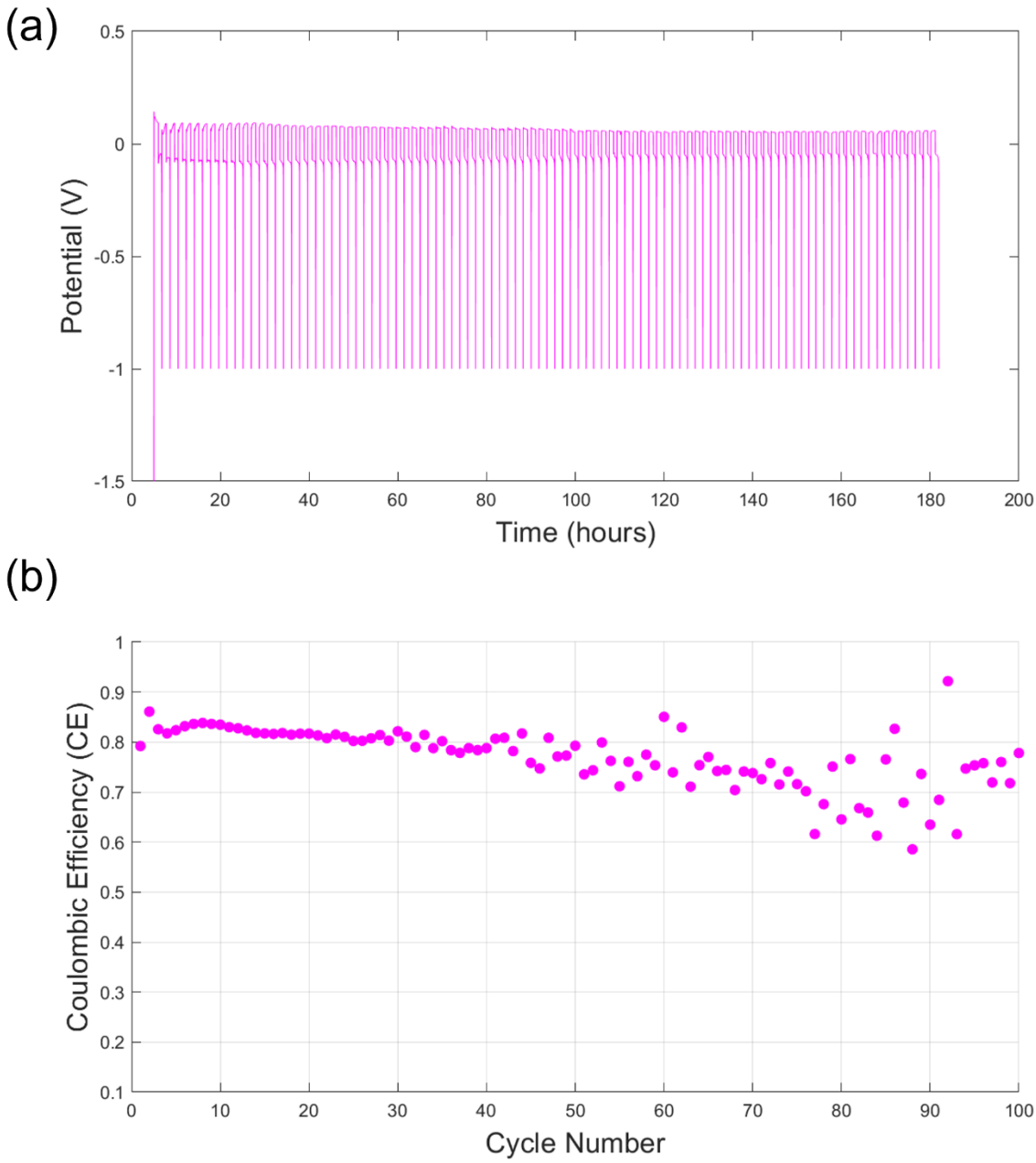

Figure S6. Example data of (a) voltage vs. time charging profile and (b) per cycle CE of a BOB^- cell used to calculate average CE shown in Figure 1. At least three cells are used to tabulate the values in Figure 1.

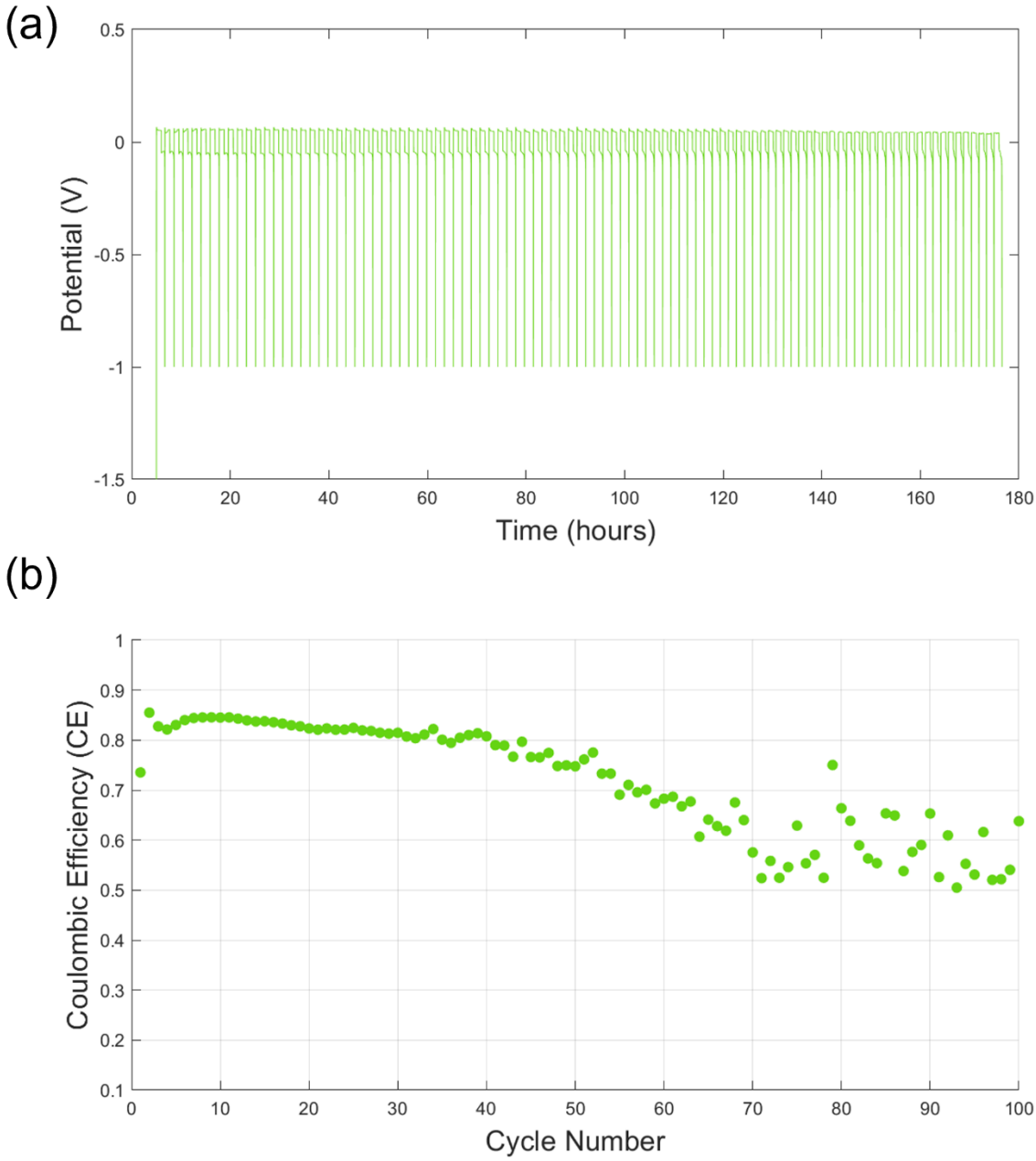

Figure S7. Example data of (a) voltage vs. time charging profile and (b) per cycle CE of a 1:1 PB cell used to calculate average CE shown in Figure 1. At least three cells are used to tabulate the values in Figure 1.

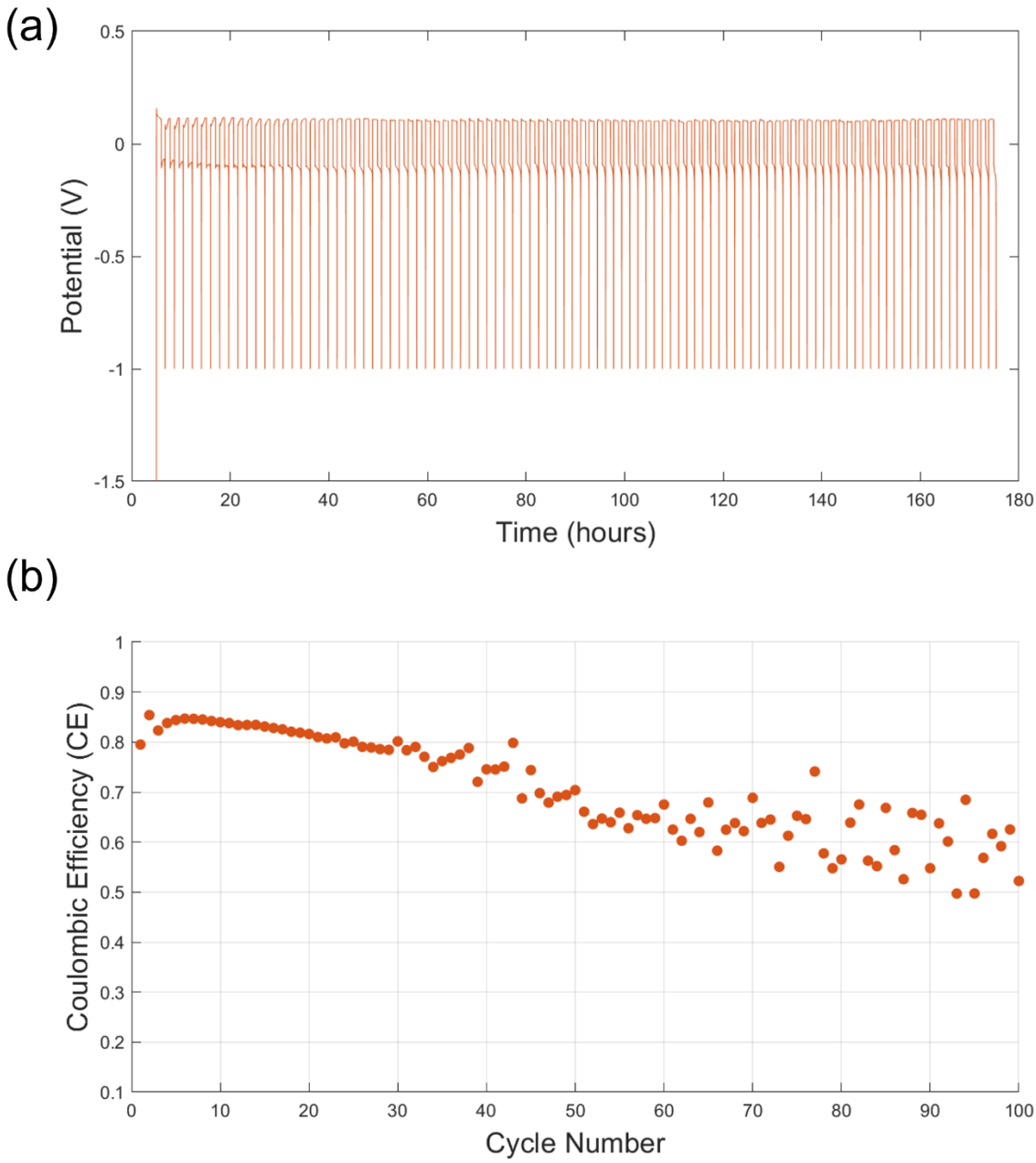

Figure S8. Example data of (a) voltage vs. time charging profile and (b) per cycle CE of a 99:1 BN cell used to calculate average CE shown in Figure 1. At least three cells are used to tabulate the values in Figure 1.

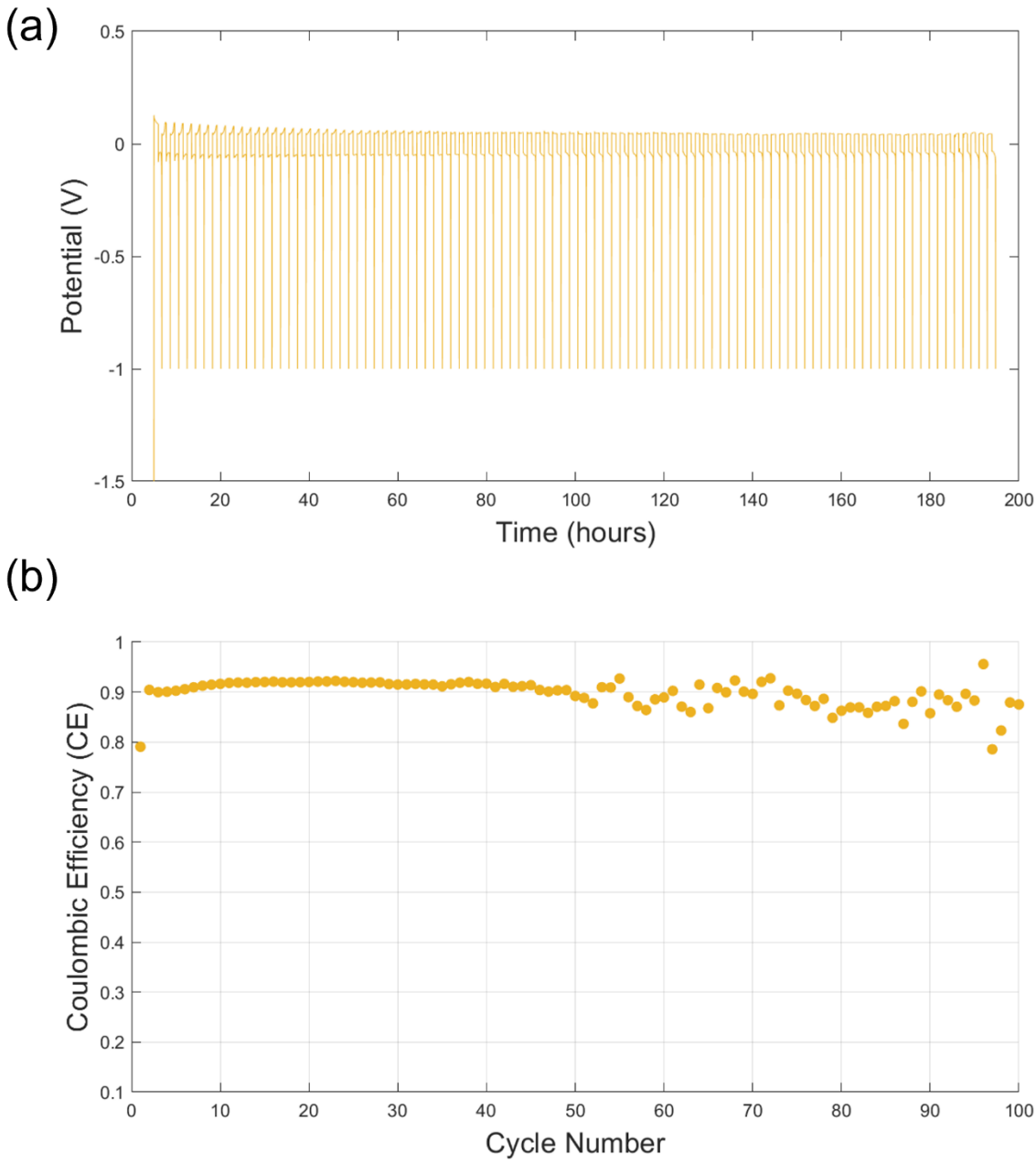

Figure S9. Example data of (a) voltage vs. time charging profile and (b) per cycle CE of a 9:1 BN cell used to calculate average CE shown in Figure 1. At least three cells are used to tabulate the values in Figure 1.

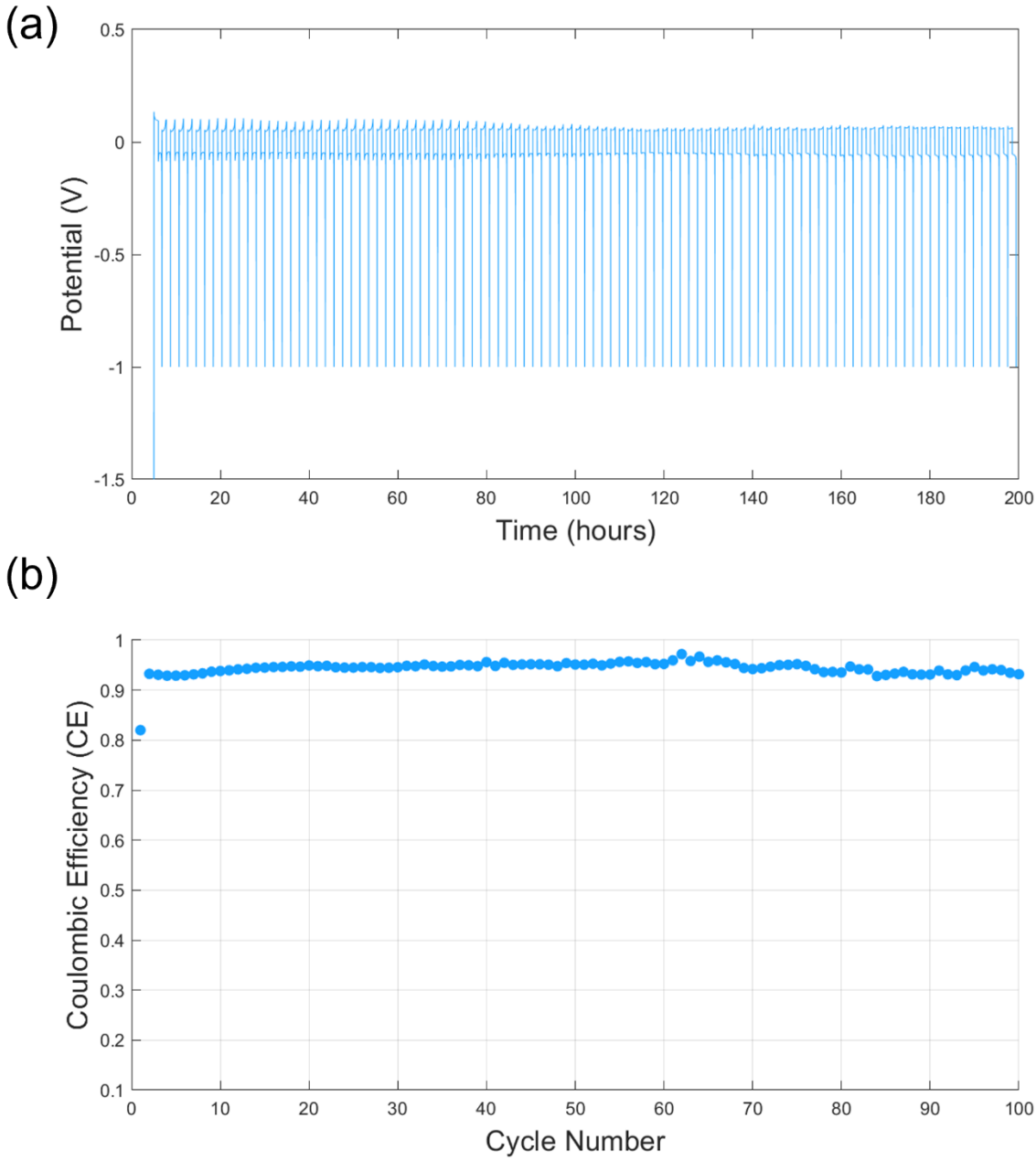

Figure S10. Example data of (a) voltage vs. time charging profile and (b) per cycle CE of a 4:1 BN cell used to calculate average CE shown in Figure 1. At least three cells are used to tabulate the values in Figure 1.

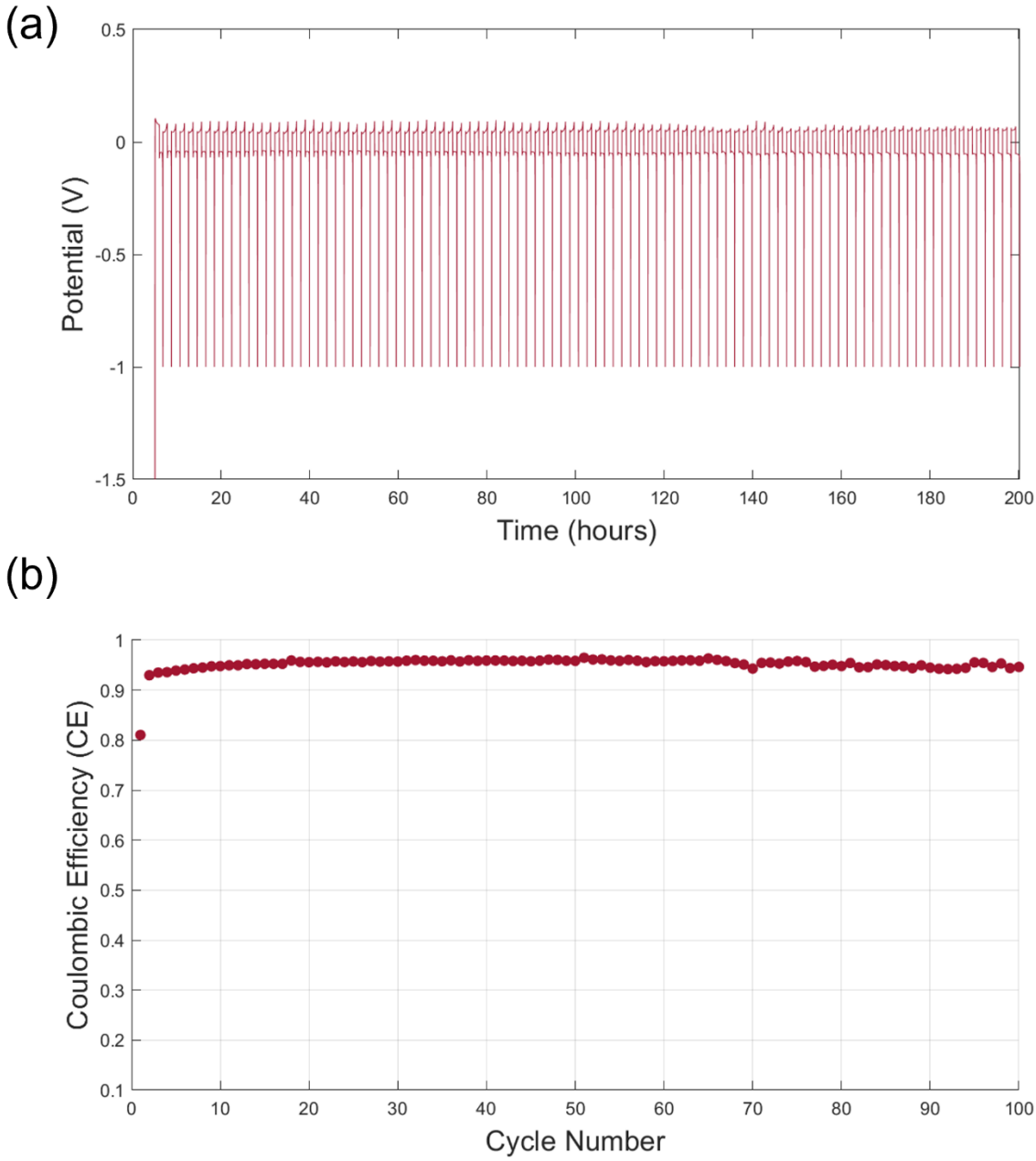

Figure S11. Example data of (a) voltage vs. time charging profile and (b) per cycle CE of a 1:1 BN cell used to calculate average CE shown in Figure 1. At least three cells are used to tabulate the values in Figure 1.

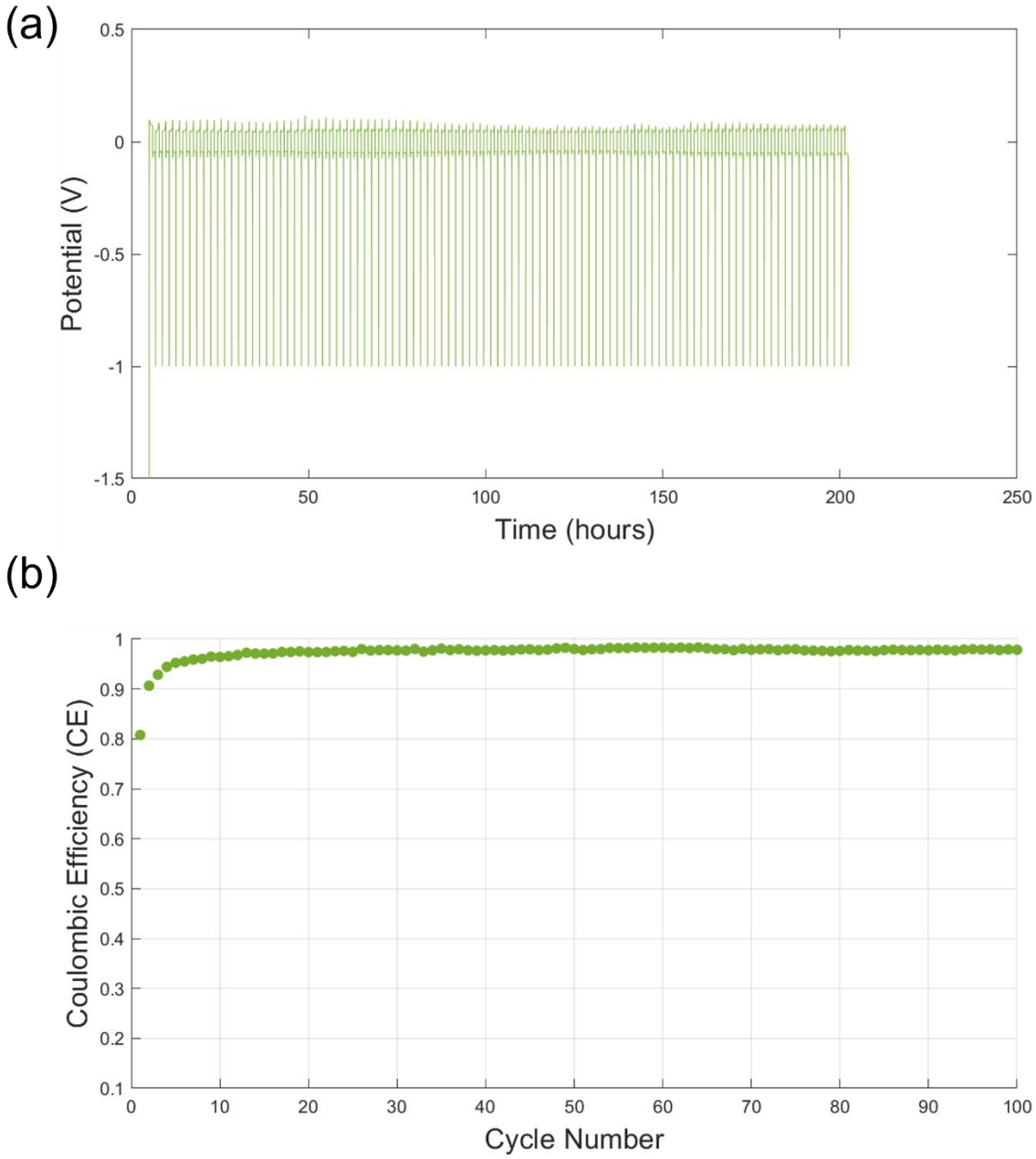

Figure S12. Example data of (a) voltage vs. time charging profile and (b) per cycle CE of a 1:4 BN cell used to calculate average CE shown in Figure 1. At least three cells are used to tabulate the values in Figure 1.

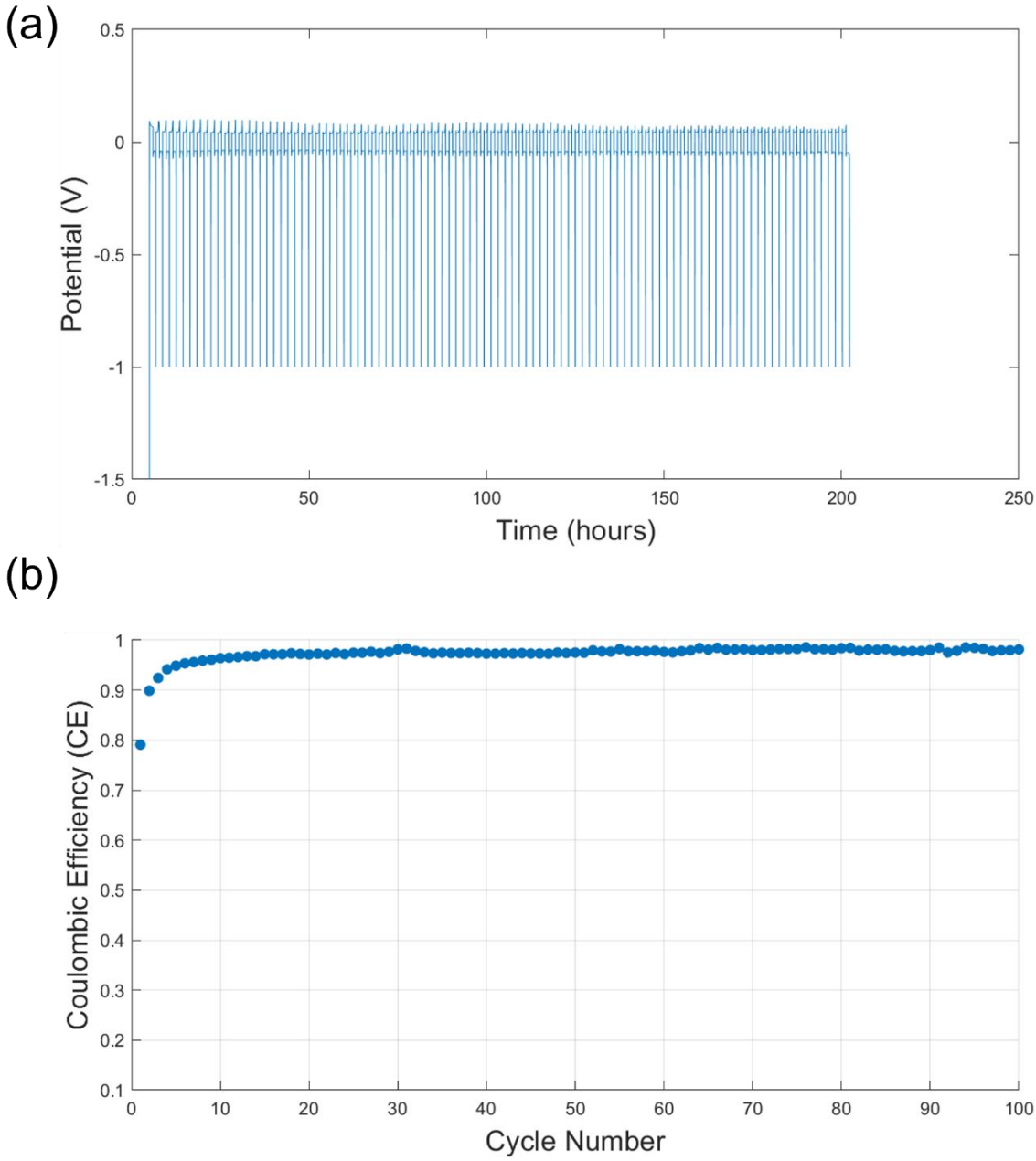

Figure S13. Example data of (a) voltage vs. time charging profile and (b) per cycle CE of a 1:9 BN cell used to calculate average CE shown in Figure 1. At least three cells are used to tabulate the values in Figure 1.

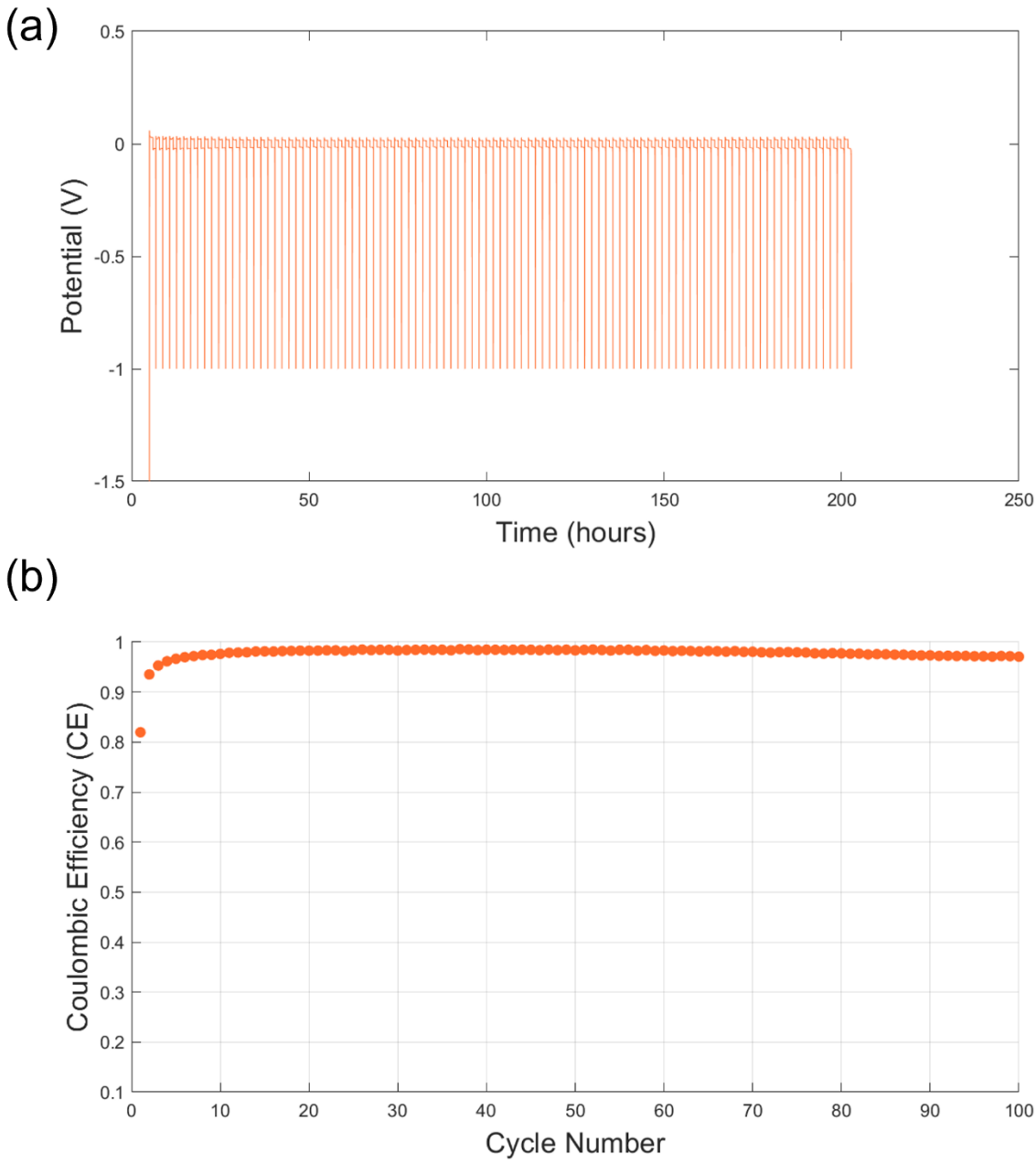

Figure S14. Example data of (a) voltage vs. time charging profile and (b) per cycle CE of a 1:1 PN cell used to calculate average CE shown in Figure 1. At least three cells are used to tabulate the values in Figure 1.

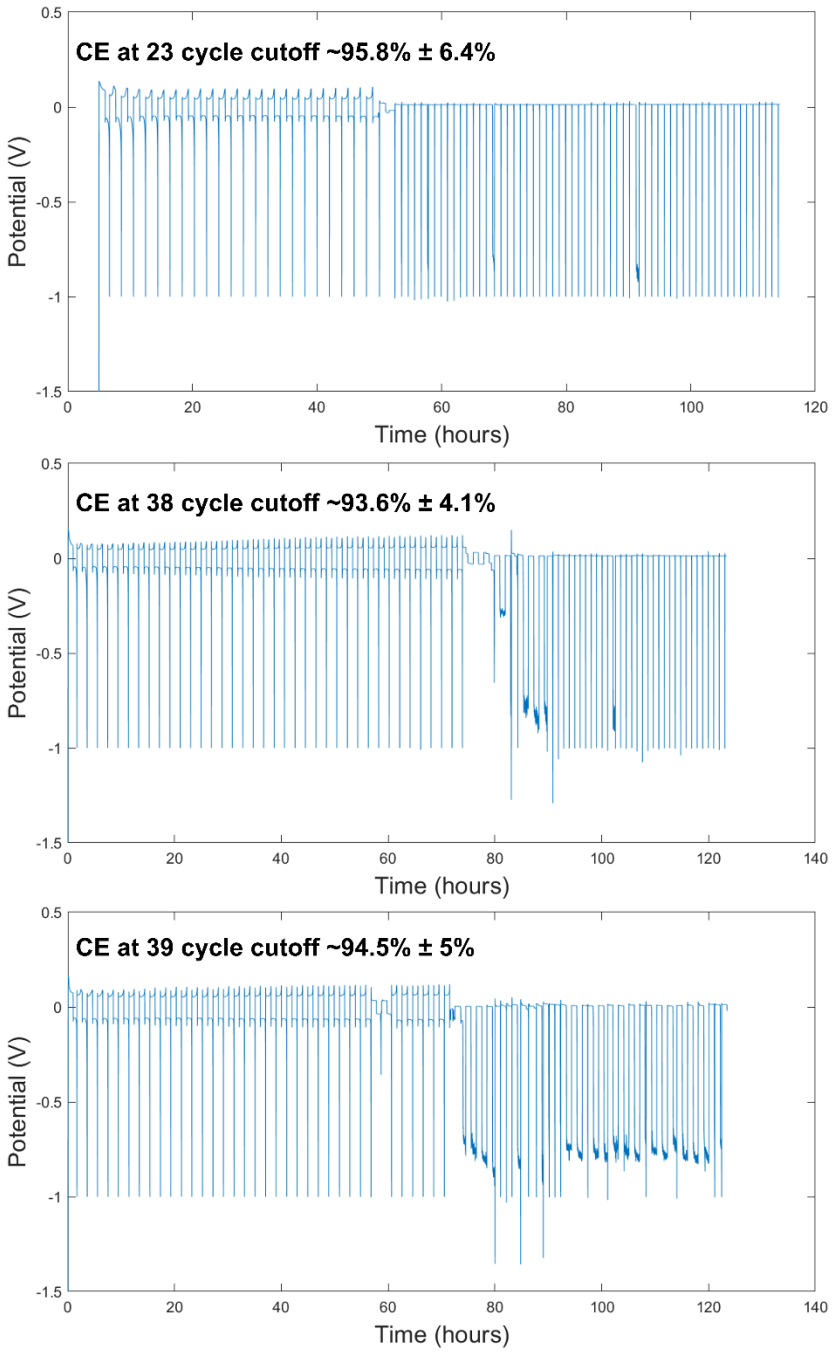

Figure S15. Three separate trials of NO_3^- charging in Cu||Li half cells. Cells consistently shorted at around 40 cycles. Labeled CE values are an average of cycle efficiency from cycle 1 until the designated cycle value which is the point of failure. Notably, until the point of failure we see relatively high values of CE, akin to the trend shown in figure 3a where more NO_3^- content corresponds with increasing CE.

Table S5. Coulombic efficiency values for Cu||Li half cells.

Tabulation of average coulombic efficiencies across cycles for 10 different cell types. Values in the table are averaged across specified cycles (either cycles 1-100 or 11-100) from at least three different cells. The standard deviation of those replicate trials is included as error.

Sample	CE cycles 1-100 (%)	CE cycles 11-100 (%)
PF_6	80.6 ± 7.1	80.1 ± 7.9
BOB	76.5 ± 1.8	75.8 ± 2
1:1 PB	71 ± 0.6	69.6 ± 0.7
99:1 BN	73.3 ± 3.9	72.5 ± 4.3
9:1 BN	90.3 ± 0.8	90.4 ± 0.9
4:1 BN	93.8 ± 0.8	94.1 ± 0.8
1:1 BN	95.4 ± 0.8	95.7 ± 0.8
1:4 BN	96.4 ± 1	97.1 ± 0.7
1:9 BN	97.1 ± 0.2	97.8 ± 0.08
1:1 PN	97.8 ± 0.5	97.8 ± 0.2

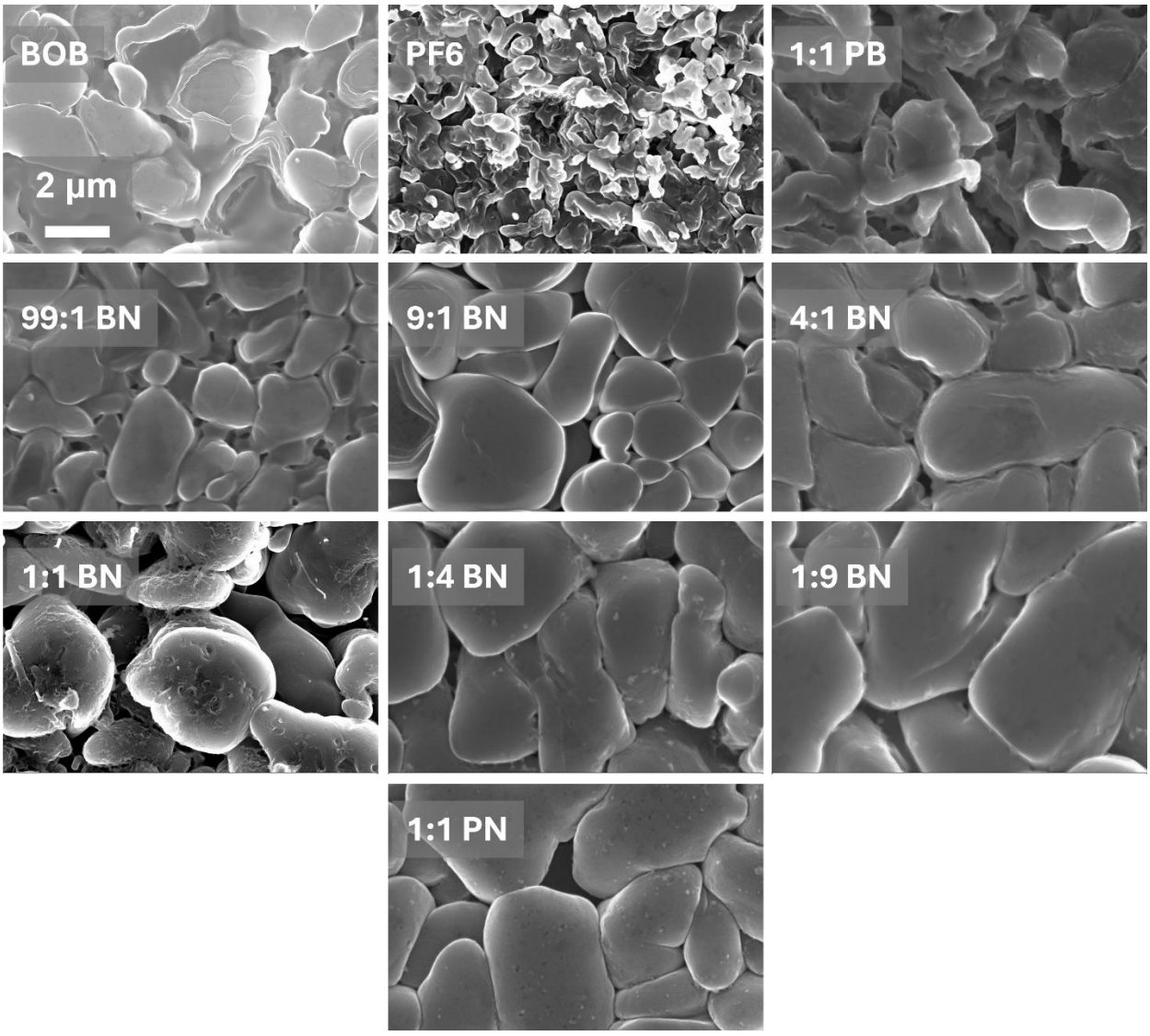

Figure S16. SEM images of the plated lithium on copper current collectors taken after applying 4 mAh/cm^2 plating capacity. Images are at a 10k magnification.

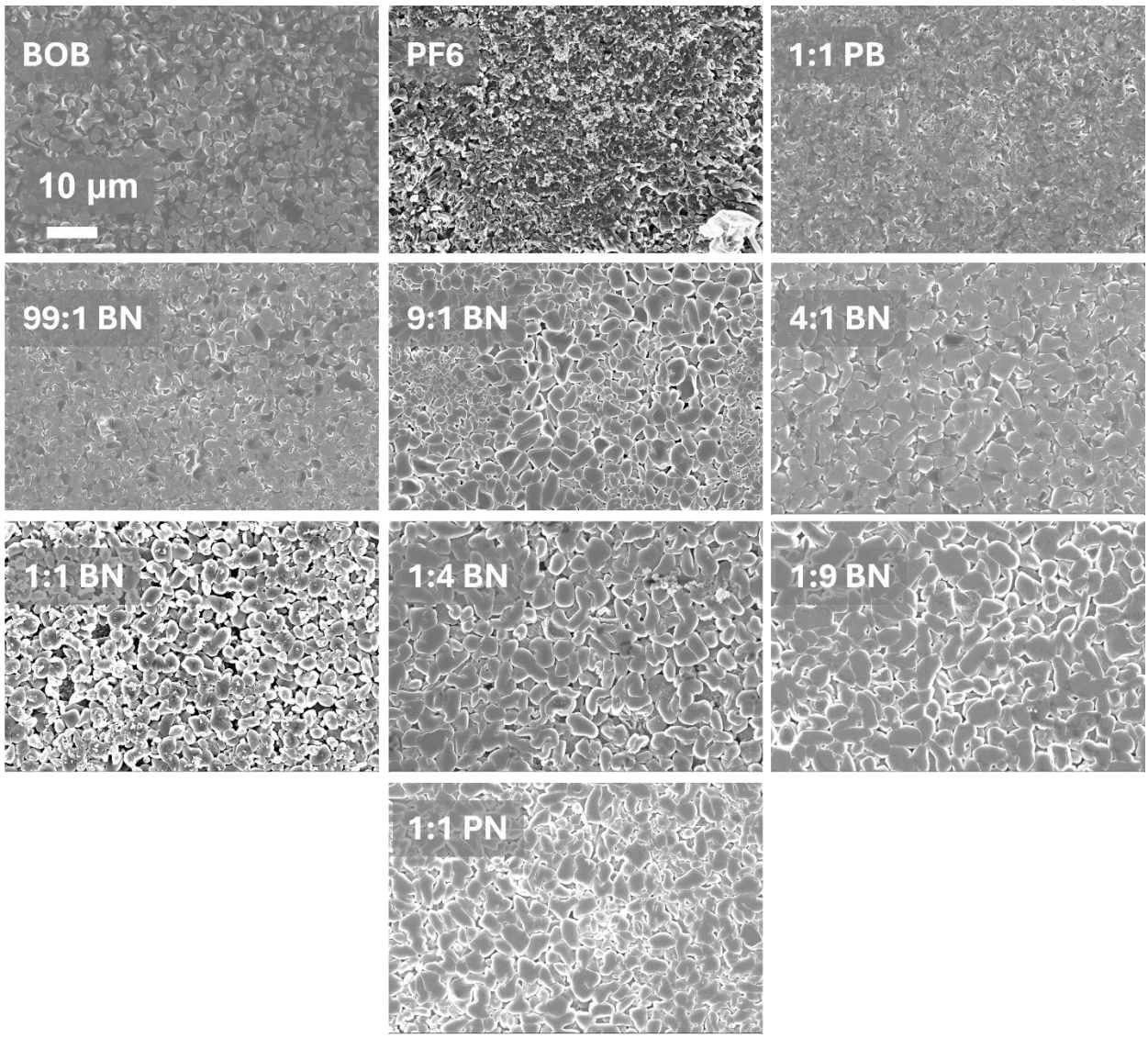

Figure S17. SEM images of the plated lithium on copper current collectors taken after applying 4 mAh/cm^2 plating capacity. Images are at a 1.5k magnification.

Table S6. XPS elemental compositional breakdown

Elemental compositional breakdown of the elemental environments present in XPS analysis. Reported values are calculated from XPS high resolution scans and survey scan averages using the MultiPak software.

Element	BOB^-	PF_6^-	NO_3^-	1:1 PB	1:1 BN	1:1 PN
C 1s	39.1%	32.2%	49.6%	37.4%	39.1%	26.8%
O 1s	44.7%	29.1%	30.6%	46.0%	47.4%	26.4%
Li 1s	12.0%	24.6%	18.8%	10.1%	6.5%	32.4%
F 1s	0%	11.8%	0%	3.0%	0%	10.8%
B 1s	3.8%	1.1%	0%	2.7%	6.2%	0.3%
P 2p	0%	1.0%	0%	0.4%	0%	0.8%
N 1s	0.4%	0.3%	1.0%	0.5%	0.9%	2.5%
Cu 2p3	0%	0%	0%	0%	0%	0%

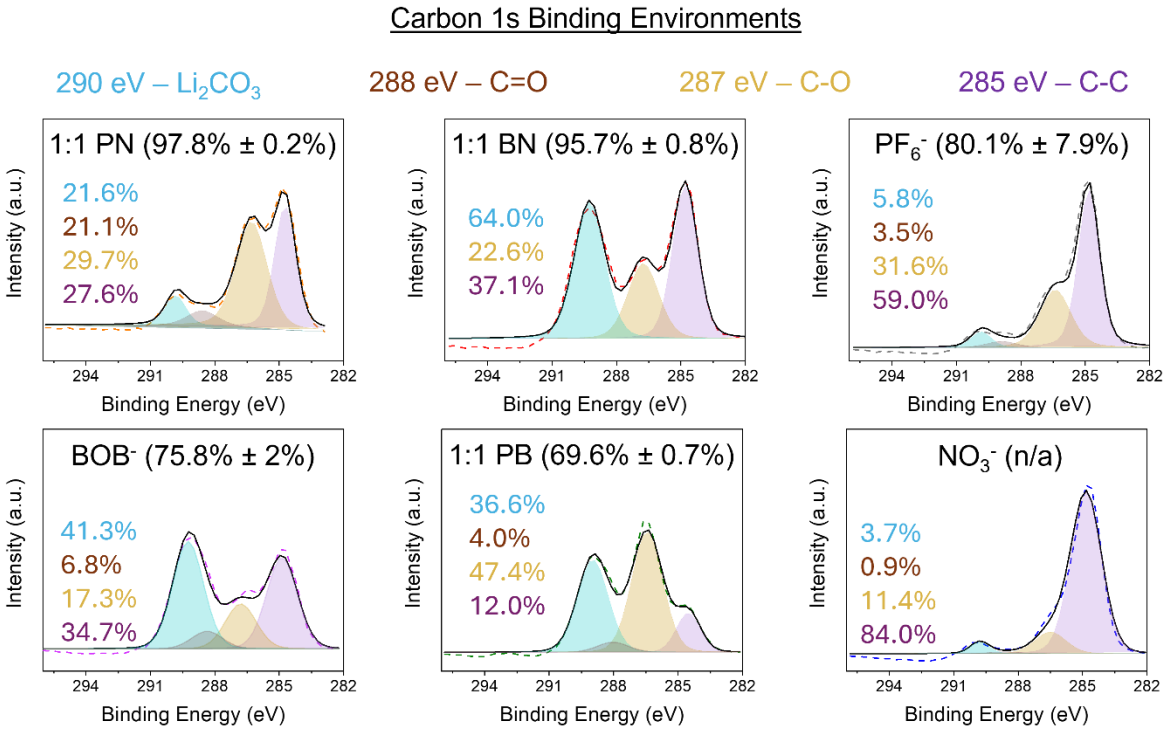

Figure S18. Carbon 1s high resolution XPS scans of six electrolyte types. Values in parentheses next to cell type label represent average CE from cycles 11-100.For all spectra, the dashed line is the raw XPS data, and the black solid line is the fitted spectra. Fittings were conducted using the Multipak software. Written percentages indicate the compositional breakdown of the color-matched carbon region. For total compositional percentage breakdown see Table S7. Spectra are referenced to adventitious carbon at 284.8 eV. This reference is kept for all following orbitals.

Table S7. XPS C 1s compositional breakdown

Carbon 1s compositional breakdown from high resolution C 1s XPS scans. Peak fitting conducted using the MultiPak software. Peak assignments were made based on literature precedent. Percent values outside of parentheses represent the percentage of the elemental environment that the specific environment makes up, while percentage values in parentheses represent the percentage the specific environment makes up out of the total SEI composition.

Binding environment	**Binding energy (eV)**	**BOB^-**	**PF_6^-**	**NO_3^-**	**1:1 PB**	**1:1 BN**	**1:1 PN**
C-C	285	34.7% (13.6%)	59.0% (19.0%)	84.0% (41.7%)	12.0% (4.5%)	37.1% (14.5%)	27.6% (7.4%)
C-O	287	17.3% (6.8%)	31.6% (12.2%)	11.4% (5.7%)	47.4% (17.7%)	22.6% (8.8%)	29.7% (8.0%)
C=O	288	6.8% (2.7%)	3.5% (1.1%)	0.9% (0.4%)	4.0% (1.5%)	0% (0%)	21.1% (5.7%)
Li_2**C**O_3	290	41.3% (16.1%)	5.8% (1.9%)	3.7% (1.8%)	36.6% (13.7%)	64.0% (25.0%)	21.6% (5.8%)

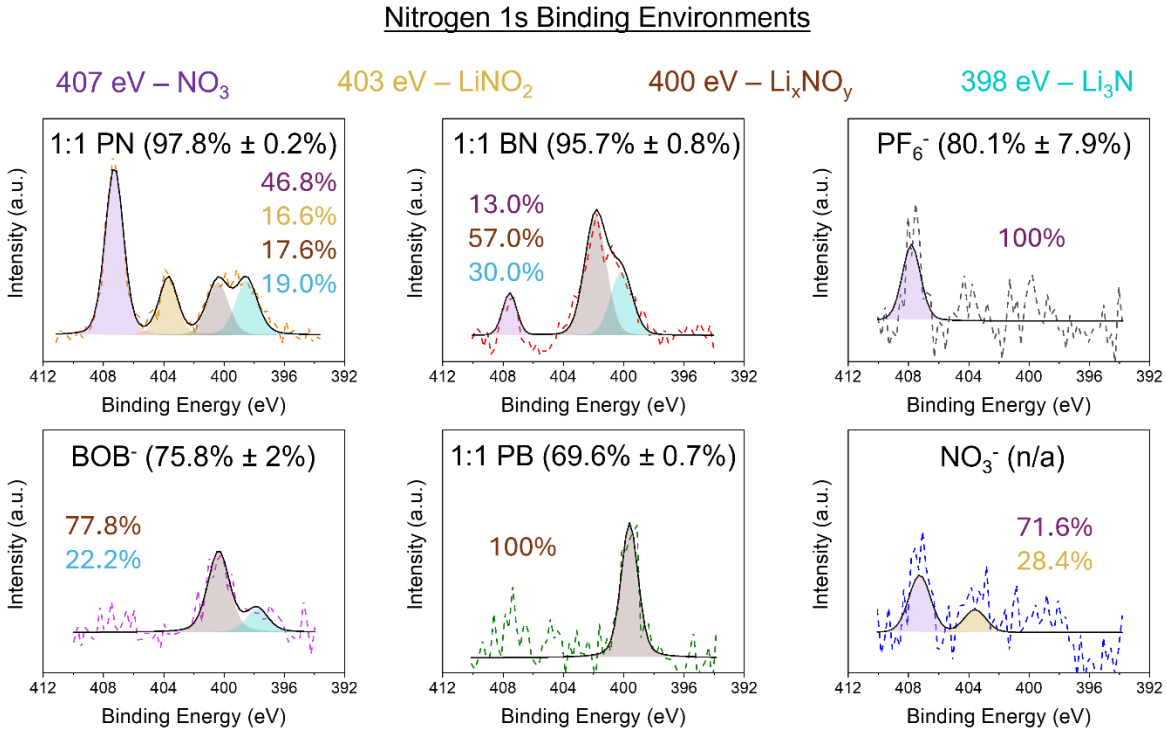

Figure S19. Nitrogen 1s high resolution XPS scans of six electrolyte types. Values in parentheses next to cell type label represent average CE from cycles 11-100. For all spectra, the dashed line is the raw XPS data, and the black solid line is the fitted spectra. Fittings were conducted using the Multipak software. Written percentages indicate the compositional breakdown of the color-matched nitrogen region. For total compositional percentage breakdown see Table S8. Inert N_2 gas within the XPS instrument is a likely source of the nitrogen environments seen in all cell types.

Table S8. XPS N 1s compositional breakdown

Nitrogen 1s compositional breakdown from high resolution N 1s XPS scans. Peak fitting conducted using the MultiPak software. Peak assignments were made based on literature precedent. Percent values outside of parentheses represent the percentage of the elemental environment that the specific environment makes up, while percentage values in parentheses represent the percentage the specific environment makes up out of the total SEI composition.

Binding environment	**Binding energy (eV)**	**BOB^-**	**PF_6^-**	**NO_3^-**	**1:1 PB**	**1:1 BN**	**1:1 PN**
$Li_3\mathbf{N}$	398	22.2% (0.1%)	0% (0%)	0% (0%)	0% (0%)	30.0% (0.3%)	19.0% (0.5%)
$Li_x\mathbf{N}O_y$	400	77.8% (0.3%)	0% (0%)	0% (0%)	100% (0.5%)	57.0% (0.5%)	17.6% (0.4%)
$Li\mathbf{N}O_2$	403	0% (0%)	0% (0%)	28.4% (0.3%)	0% (0%)	0%	16.6% (0.4%)
$\mathbf{N}O_3$	407	0% (0%)	100% (0.3%)	71.6% (0.7%)	0% (0%)	13.0% (0.1%)	46.8% (1.2%)

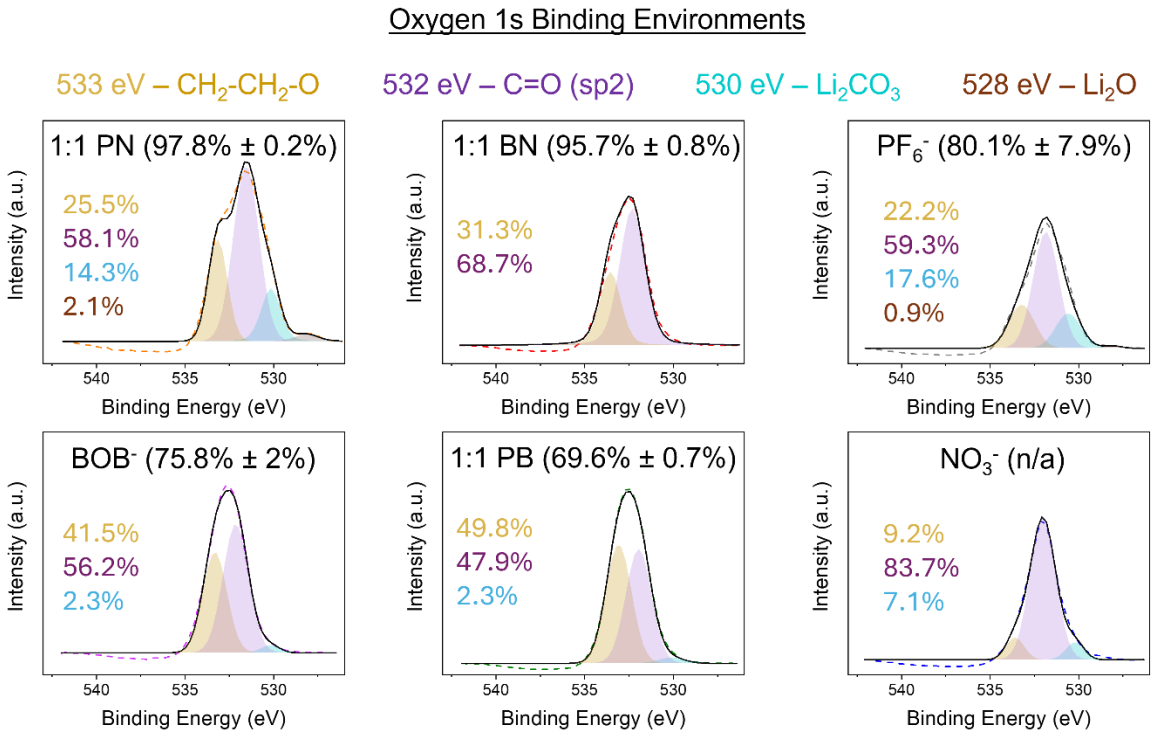

Figure S20. Oxygen 1s high resolution XPS scans of six electrolyte types. Values in parentheses next to cell type label represent average CE from cycles 11-100. For all spectra, the dashed line is the raw XPS data, and the black solid line is the fitted spectra. Fittings were conducted using the Multipak software. Written percentages indicate the compositional breakdown of the color-matched oxygen region. For total compositional percentage breakdown see Table S9.

Table S9. XPS O 1s compositional breakdown

Oxygen 1s compositional breakdown from high resolution O 1s XPS scans. Peak fitting conducted using the MultiPak software. Peak assignments were made based on literature precedent. Percent values outside of parentheses represent the percentage of the elemental environment that the specific environment makes up, while percentage values in parentheses represent the percentage the specific environment makes up out of the total SEI composition.

Binding environment	**Binding energy (eV)**	**BOB^-**	**PF_6^-**	**NO_3^-**	**1:1 PB**	**1:1 BN**	**1:1 PN**
Li_2**O**	528	0% (0%)	0.9% (0.3%)	0% (0%)	0% (0%)	0% (0%)	2.1% (0.6%)
Li_2C**O_3**	530	2.3% (1.0%)	17.6% (5.1%)	7.1% (2.2%)	2.3% (1.1%)	0% (0%)	14.3% (3.8%)
C=**O**	532	56.2% (25.1%)	59.3% (17.3%)	83.7% (25.6%)	47.9% (22.0%)	68.7% (32.6%)	58.1% (15.3%)
CH_2-CH_2-**O**	533	41.5% (18.6%)	22.2% (6.5%)	9.2% (2.8%)	49.8% (22.9%)	31.3% (14.8%)	25.5% (6.7%)

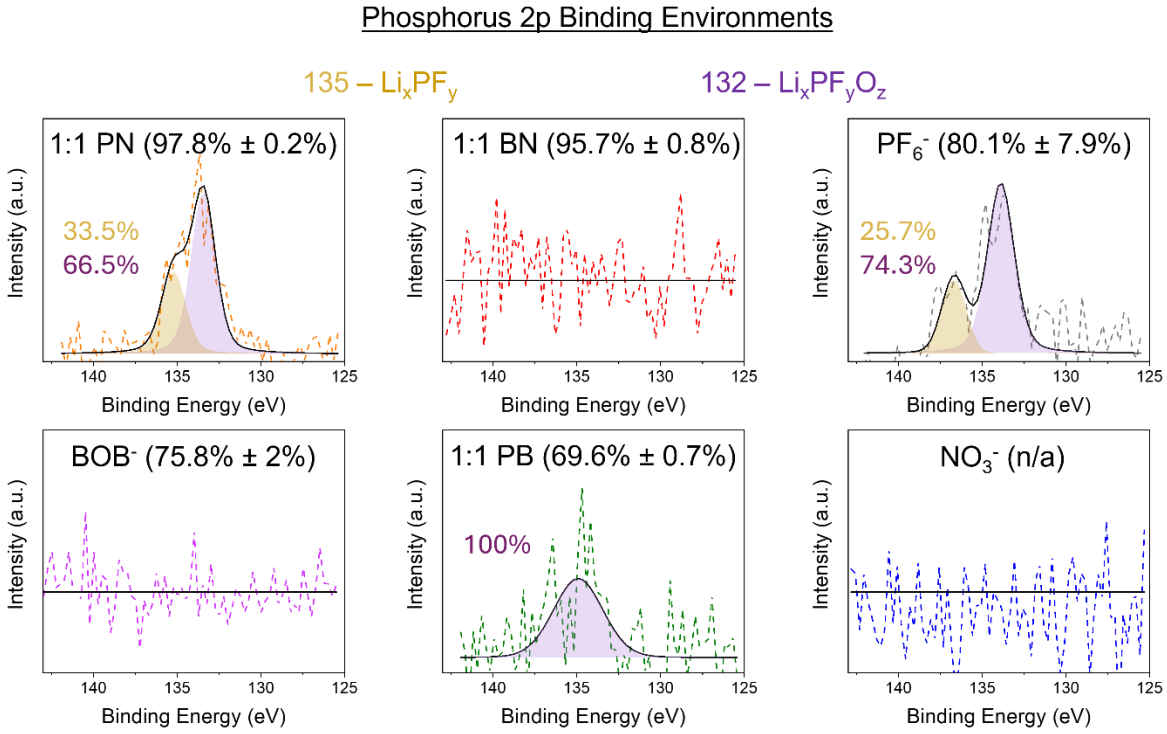

Figure S21. Phosphorus 2p high resolution XPS scans of six electrolyte types. Values in parentheses next to cell type label represent average CE from cycles 11-100. For all spectra, the dashed line is the raw XPS data, and the black solid line is the fitted spectra. Fittings were conducted using the Multipak software. Written percentages indicate the compositional breakdown of the color-matched phosphorus region. For total compositional percentage breakdown see Table S10.

Table S10. XPS P 2p compositional breakdown

Phosphorus 2p compositional breakdown from high resolution P 2p XPS scans. Peak fitting conducted using the MultiPak software. Peak assignments were made based on literature precedent. Percent values outside of parentheses represent the percentage of the elemental environment that the specific environment makes up, while percentage values in parentheses represent the percentage the specific environment makes up out of the total SEI composition.

Binding environment	**Binding energy (eV)**	**BOB^-**	**PF_6^-**	**NO_3^-**	**1:1 PB**	**1:1 BN**	**1:1 PN**
$Li_xPF_yO_z$	132	0% (0%)	74.3% (0.7%)	0% (0%)	100% (0.4%)	0% (0%)	66.5% (0.5%)
Li_xPF_y	135	0% (0%)	25.7% (<0.3%)	0% (0%)	0% (0%)	0% (0%)	33.5% (0.3%)

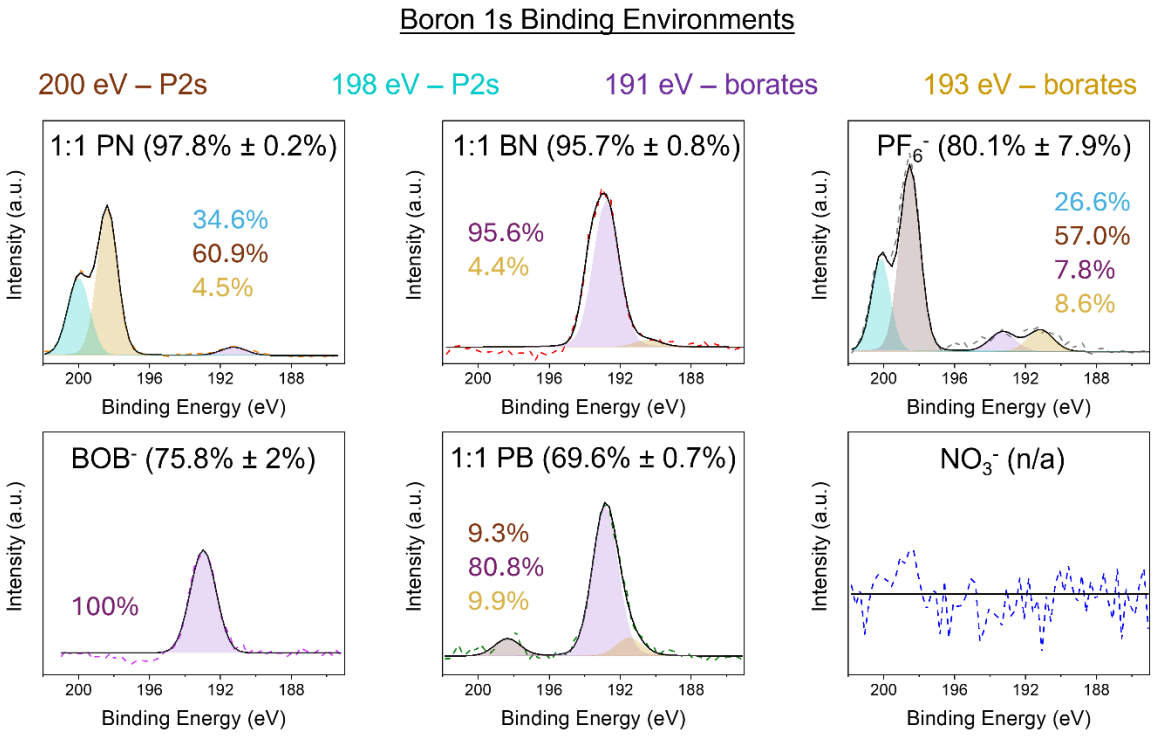

Figure S22. Boron 1s high resolution XPS scans of six electrolyte types. Values in parentheses next to cell type label represent average CE from cycles 11-100. For all spectra, the dashed line is the raw XPS data, and the black solid line is the fitted spectra. Fittings were conducted using the Multipak software. Written percentages indicate the compositional breakdown of the color-matched boron (or P 2s) region. For total compositional percentage breakdown see Table S11.

Table S11. XPS B 1s compositional breakdown

Boron 1s compositional breakdown from high resolution B 1s XPS scans. Peak fitting conducted using the MultiPak software. Peak assignments were made based on literature precedent. Percent values outside of parentheses represent the percentage of the elemental environment that the specific environment makes up, while percentage values in parentheses represent the percentage the specific environment makes up out of the total SEI composition.

Binding environment	Binding energy (eV)	BOB^-	PF_6^-	NO_3^-	1:1 PB	1:1 BN	1:1 PN
Borates type 1	191	0% (0%)	8.6% (0.6%)	0% (0%)	9.9% (3%)	4.4% (0.3%)	4.5% (0.3%)
Borates type 2	193	100% (3.8%)	7.8% (0.5%)	0% (0%)	80.8% (2.4%)	95.6% (5.9%)	0%
P2s	198	0% (0%)	57.0%	0% (0%)	0%	0%	60.9%
P2s	200	0% (0%)	26.6%	0% (0%)	9.3%	0%	34.6%

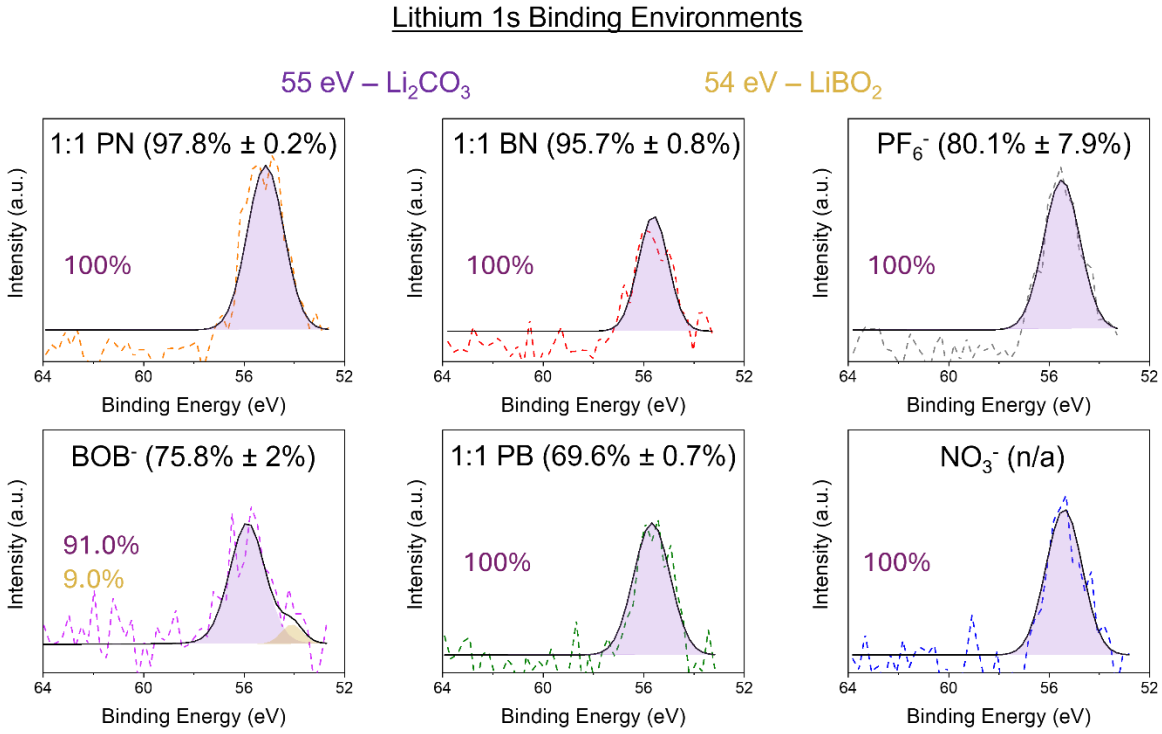

Figure S23. Lithium 1s high resolution XPS scans of six electrolyte types. Values in parentheses next to cell type label represent average CE from cycles 11-100. For all spectra, the dashed line is the raw XPS data, and the black solid line is the fitted spectra. Fittings were conducted using the Multipak software. Written percentages indicate the compositional breakdown of the color-matched lithium region. For total compositional percentage breakdown see Table S12.

Table S12. XPS Li 1s compositional breakdown

Lithium 1s compositional breakdown from high resolution Li 1s XPS scans. Peak fitting conducted using the MultiPak software. Peak assignments were made based on literature precedent. Percent values outside of parentheses represent the percentage of the elemental environment that the specific environment makes up, while percentage values in parentheses represent the percentage the specific environment makes up out of the total SEI composition.

Binding environment	Binding energy (eV)	BOB^-	PF_6^-	NO_3^-	1:1 PB	1:1 BN	1:1 PN
LiBO_2	54	9.0% (1.1%)	0% (0%)	0% (0%)	0% (0%)	0% (0%)	0% (0%)
Li$_2CO_3$	55	91.0% (10.9%)	100% (24.6%)	100% (18.8%)	100% (10.1%)	100% (6.5%)	100% (32.4)

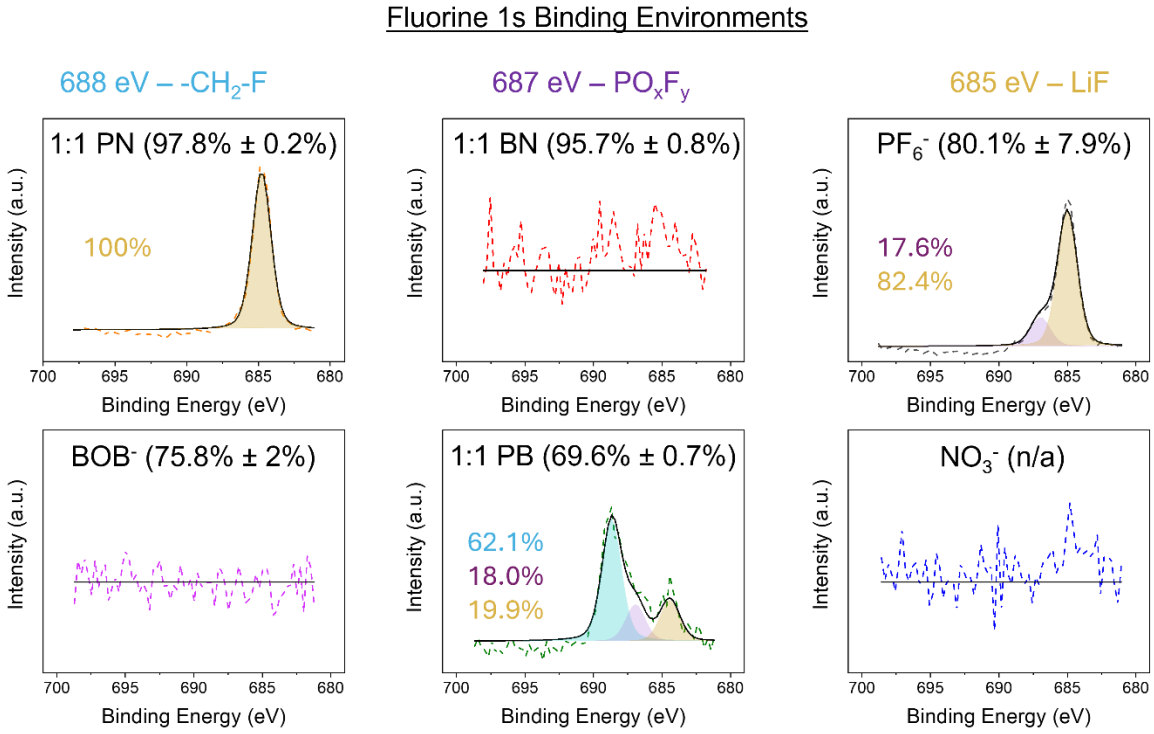

Figure S24. Fluorine 1s high resolution XPS scans of six electrolyte types. Values in parentheses next to cell type label represent average CE from cycles 11-100. For all spectra, the dashed line is the raw XPS data, and the black solid line is the fitted spectra. Fittings were conducted using the Multipak software. Written percentages indicate the compositional breakdown of the color-matched fluorine region. For total compositional percentage breakdown see Table S13.

Table S13. XPS F 1s compositional breakdown

Fluorine 1s compositional breakdown from high resolution F 1s XPS scans. Peak fitting conducted using the MultiPak software. Peak assignments were made based on literature precedent. Percent values outside of parentheses represent the percentage of the elemental environment that the specific environment makes up, while percentage values in parentheses represent the percentage the specific environment makes up out of the total SEI composition.

Binding environment	**Binding energy (eV)**	**BOB^-**	**PF_6^-**	**NO_3^-**	**1:1 PB**	**1:1 BN**	**1:1 PN**
Li**F**	685	0% (0%)	82.4% (9.7%)	0% (0%)	19.9% (0.6%)	0% (0%)	27.6% (3.0%)
$PO_x\mathbf{F}_y$	687	0% (0%)	17.6% (2.1%)	0% (0%)	18.0% (0.5%)	0% (0%)	29.7% (3.2%)
-CH_2-**F**	688	0% (0%)	0% (0%)	0% (0%)	62.1% (1.9%)	0% (0%)	0% (0%)

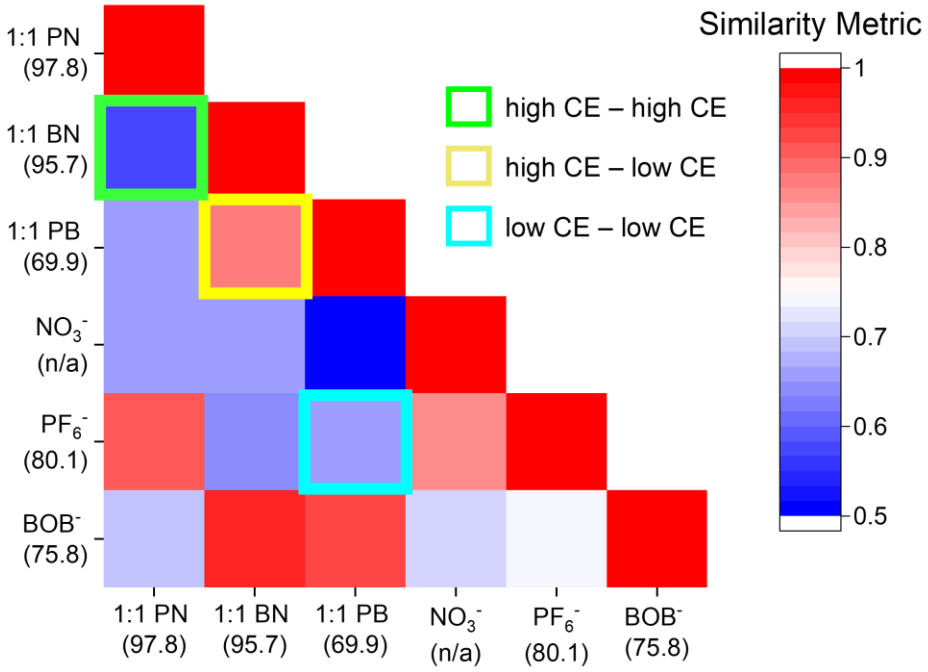

Figure S25. Cosine similarity of XPS compositions calculated for the 21 comparative cell to cell combinations. A value closer to 1 (red) indicates high similarity, and a value closer to 0.5 (blue) indicates low similarity. The green box highlights the similarity score between 1:1 BN and 1:1 PN, the yellow box highlights the similarity score between 1:1 PB and 1:1 BN. The cyan box highlights the similarity score between PF_6^- and 1:1 PB.

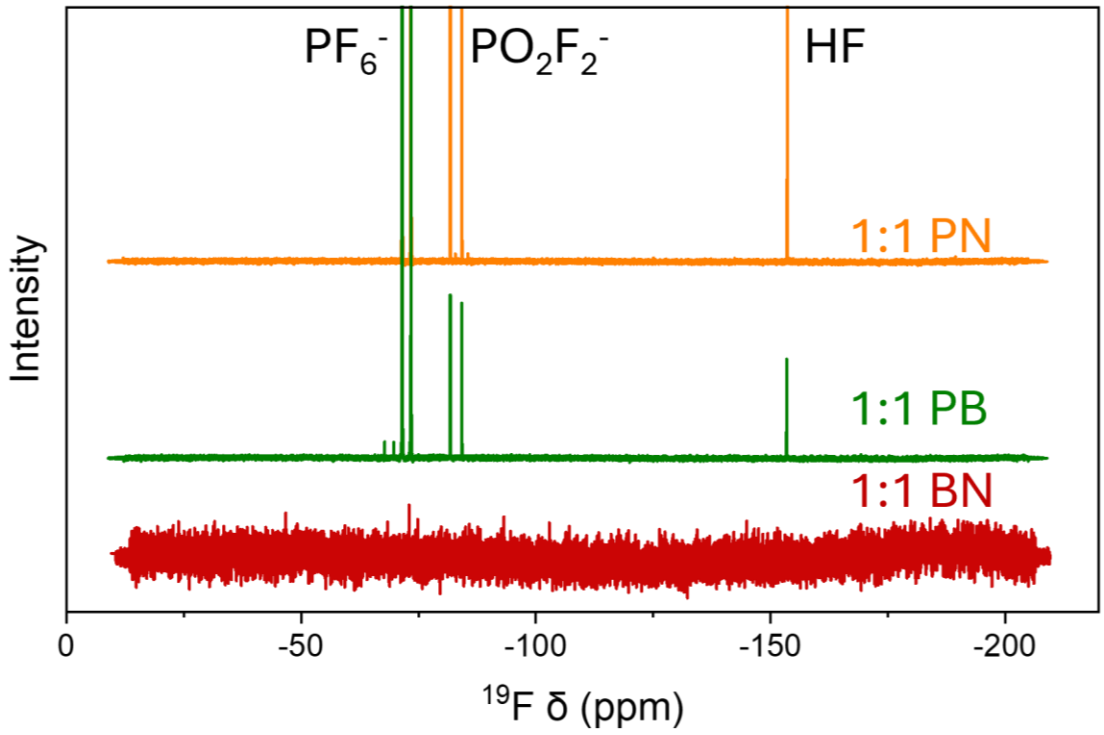

Figure S26. ^{19}F NMR acquired on at 400 MHz of the mixed salt systems 1:1 PN (orange), 1:1 PB (green), and 1:1 BN (red). Labeled peaks indicate the presence of the PF_6^- anion and decomposition products, $PO_2F_2^-$ and HF, in the 1:1 PN and 1:1 PB samples. We do not detect any fluorine-containing species in the 1:1 BN electrolyte (bottom, red).

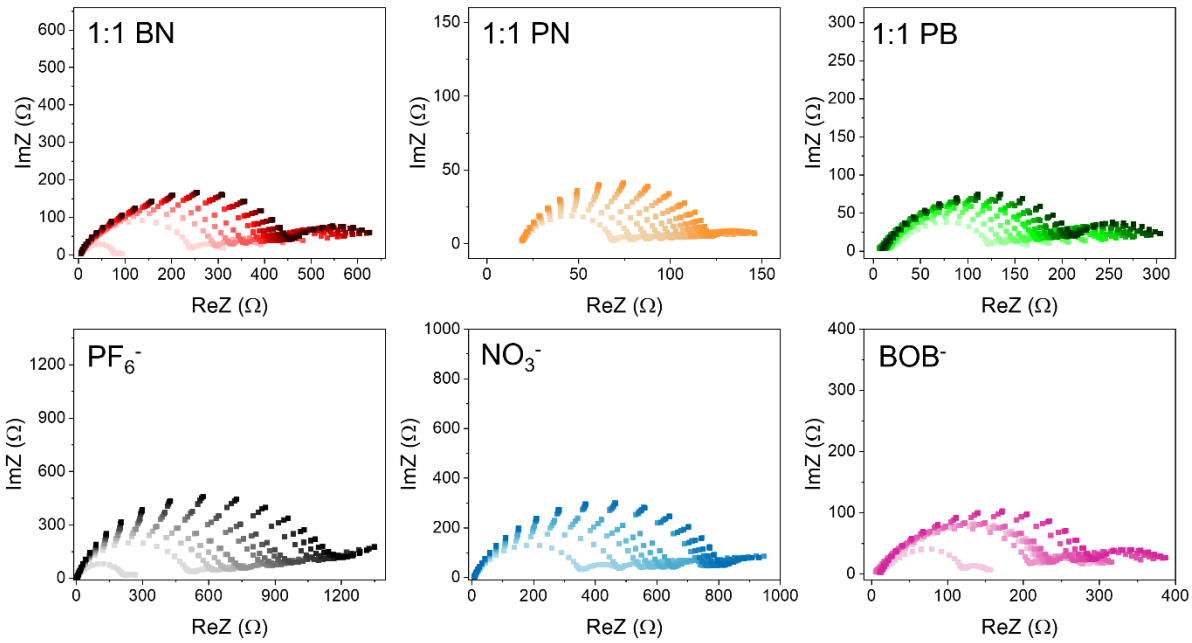

Figure S27. Example nPEIS scans from six cell types. Scans darken in color as a function of time such that the initial scan at time 0 h is the lightest color in the graph and scans at time 65 h are the darkest color in the graph. In all cell types, the Nyquist plots increase in both resistance and capacitance as a function of time. Note the difference in scale between plots for different electrolyte formulations.

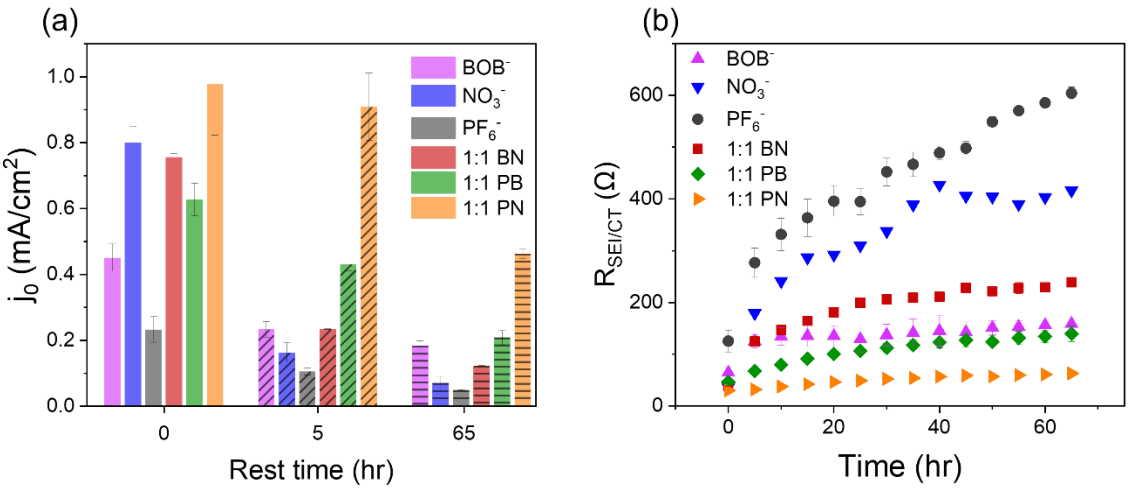

Figure S28. nPEIS results processed to show (a) calculated j_0 values extrapolated for each cell type at time 0 h (left, solid), 5 h (middle, diagonal dashed), and 65 h (right, horizontal dashed). (b) Fitted R values from EIS scans taken at each time point. In nPEIS this R value comes from a combination of charge transfer and transport through the SEI and is thus labeled as $R_{SEI/CT}$. Plotted values represent averages taken over at least three cells. The average of these replicate runs is reflected in the error bars in (a) and (b).

Table S14. j_0 values calculated from different electrochemistry methods

Calculated j_0 values reported in mA/cm^2 for each electrochemical method of measurement. CV j_0 values are normalized for each electrode to PF_6 to account for slight variations in electrode area. Three electrode results were average per sample. Three Li||Li symmetric cells were averaged for EIS measurements. The standard deviation between these replicate experiments is represented as the error values. Values represent midpoints of the experiment.

Sample	CV j_0	nPEIS 5 hr	nPEIS 65 hr	ePEIS 30 min
PF_6	1	0.1 ±0.01	0.05 ±0.001	0.8 ±0.1
BOB	1.1 ±0.3	0.2 ±0.02	0.2 ±0.01	0.5 ±0.03
NO_3	0.9 ±0.1	0.2 ± 0.03	0.07 ±0.02	0.5 ±0.05
PB	1.4 ±0.2	0.4 ±0.02	0.2 ±0.02	0.7 ±0.04
PN	3.0 ±0.3	0.9 ±0.1	0.5 ±0.02	1.6 ±0.02
BN	3.2 ±0.4	0.2 ±0.001	0.1 ±0.001	0.6 ±0.07

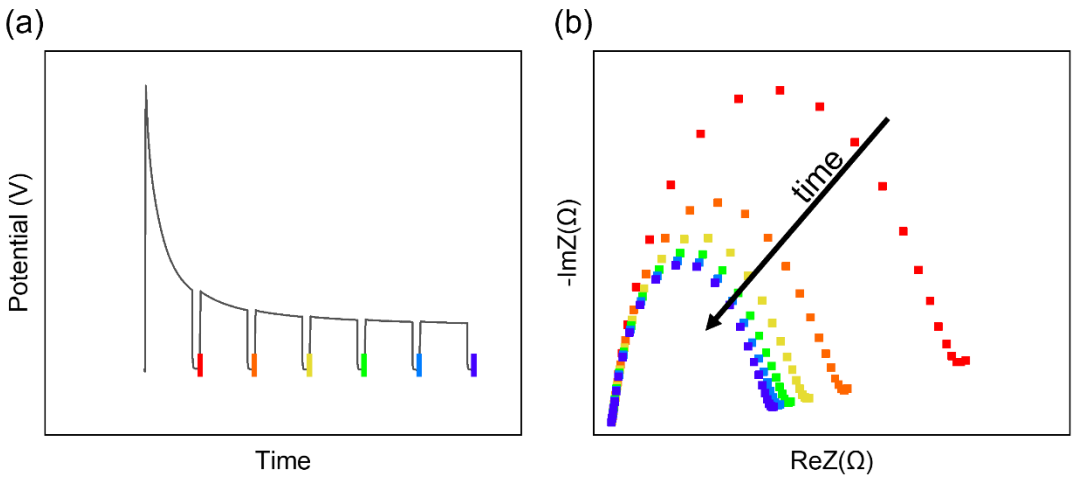

Figure S29. Schematic showing the time points of measurement during an ePEIS experiment. (a) Potential vs. time graph. After a specified time of charging (here 10 minutes) the applied current is turned off, and the cell is allowed to rest for a specified amount of time (here 1 minute) before the ePEIS measurement is taken (time of acquisition is represented by a colored marker). (b) Example Nyquist data collected from this experiment. In all cell types analyzed in this electrolyte series the resistance and capacitance decreased with charge capacity (and thus time) in the ePEIS experiment. The color of the Nyquist plot matches and represents the time of measurement.

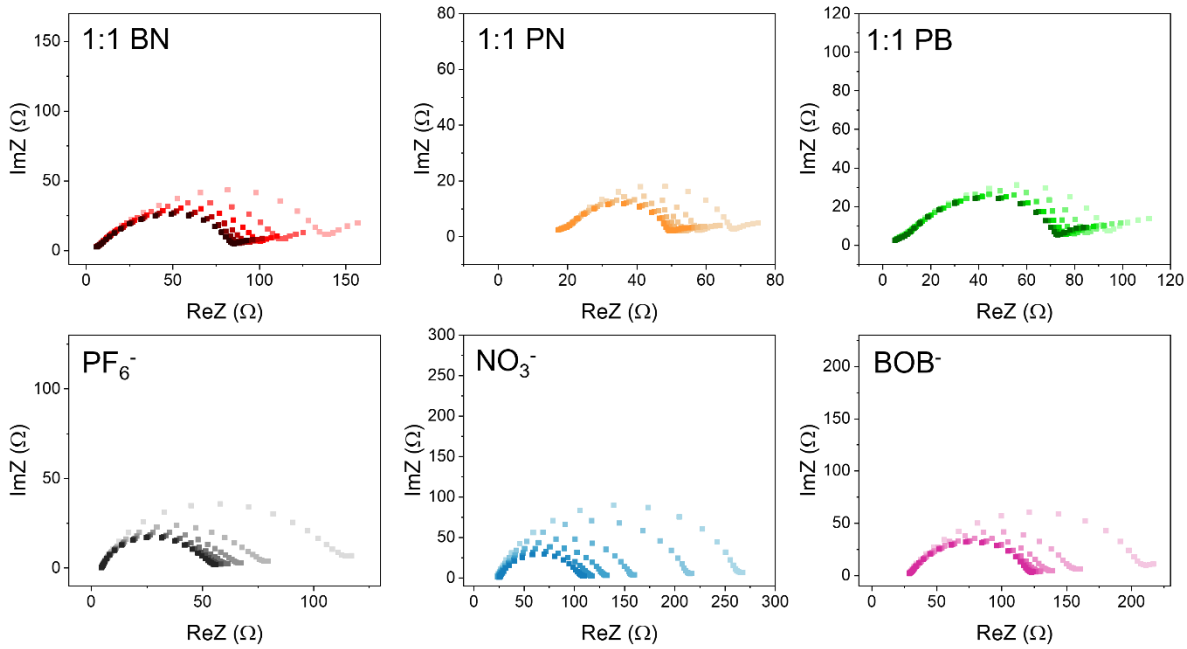

Figure S30. Example ePEIS scans from six cell types. Scans darken in color with time such that the initial scan after 10 minutes of charging is the lightest color in the graph and scans after 60 minutes of charging are the darkest color in the graph. In all cell types, the Nyquist plots decrease in both resistance and capacitance as a function of time. Note the difference in scale between plots.

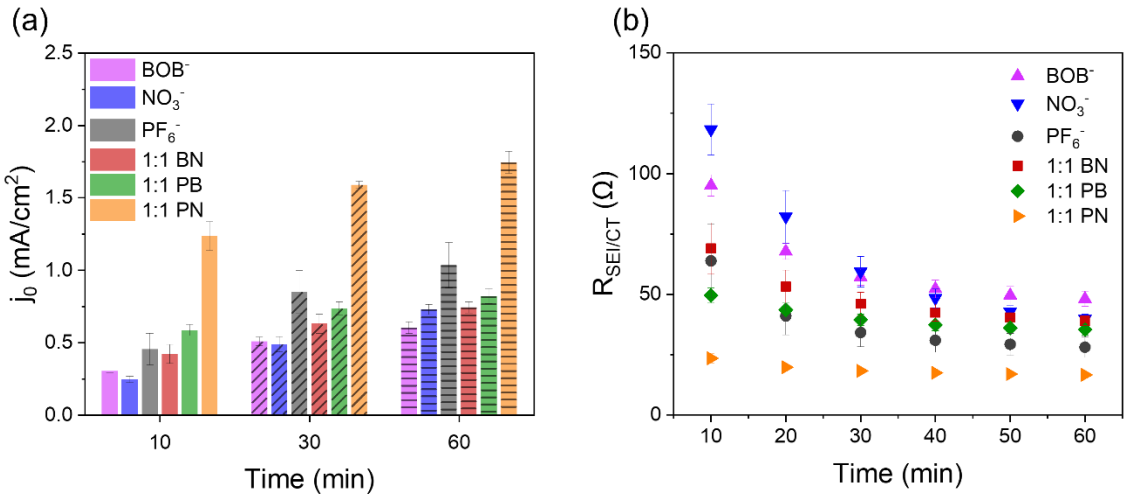

Figure S31. ePEIS results processed to show (a) calculated j_0 values extrapolated for each cell type after 10 minutes of charge (left, solid), 30 minutes of charge (middle, diagonal dashed), and 60 minutes of charge (right, horizontal dashed). (b) Fitted R value from eEIS scans taken at each time point. In ePEIS this R value comes from charge transfer and transport through the SEI and is thus labeled as $R_{SEI/CT}$. Plotted values represent averages taken over at least three cells. The average of these replicate runs is reflected in the error bars in (a) and (b).

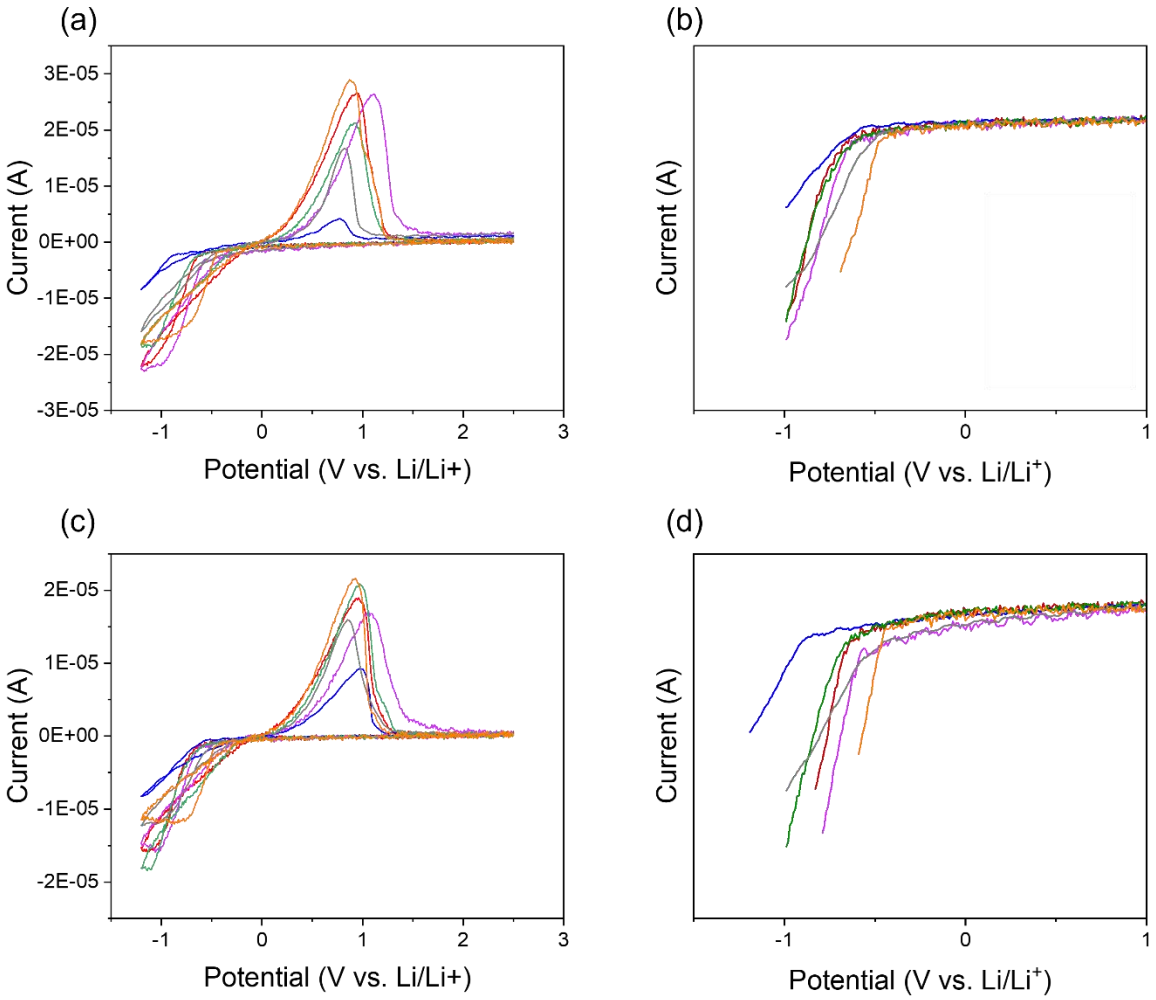

Figure S32. CV exemplary data of the lithium plating/stripping reaction taken using a tungsten UME working electrode and a lithium metal counter/reference electrode at scan rates of 10 V/s. (a) and (c) show the full voltammograms while (b) and (d) show just the plating portion of the voltammogram. In all figures, the color scheme follows that of fig. S32 where BOB^- is pink, NO_3^- is blue, PF_6^- is grey, 1:1 BN is red, 1:1 PN is orange, and 1:1 PB is green.

References

(1) Bard, A. J.; Faulkner, L. R. *Electrochemical Methods Fundamentals and Applications second edition*; 2001.

(2) Boyle, D.; Kim, S.; Oyakhire, S.; Vilá, R.; Huang, Z.; Sayavong, P.; Qin, J.; Bao, Z.; Cui, Y. Correlating Kinetics to Cyclability Reveals Thermodynamic Origin of Lithium Anode Morphology in Liquid Electrolytes. *J. Am. Chem. Soc.,* **2022**, *144*, 20717-20725.

(3) Park, S.; Sadowski, J.; Kwon, Y.; Metlay, A.; Marbella, L. Electrolyte Vapor Induced Passivation and Transition Metal Redox on Electrode Active Materials. *J. Phys. Chem. C,* **2025**, *129* (47), 20867-20879.

(4) Boyle, D.; Kong, X.; Pei, A.; Rudnicki, P.; Shi, F.; Huang, W.; Bao, Z.; Qin, J.; Cui, Y. Transient Voltammetry with Ultramicroelectrodes Reveals the Electron Transfer Kinetics of Lithium Metal Anodes. *ACS Energy Lett.* **2020**, *5*, 701-709.

(5) Oyakhire, S.; Gong, H.; Cui, Y.; Bao, Z.; Bent, S. An X-ray Photoelectron Spectroscopy Primer for Solid Electrolyte Interphase Characterization in Lithium Metal Anodes. *ACS Energy Lett.* **2022**, *7* (8).